Journal of Mammalogy, 100(4):1112–1129, 2019
DOI:10.1093/jmammal/gyz066
Version of Record, first published online 6 June 2019, with fixed content and layout in compliance with Art. 8.1.3.2 ICZN.

Two new species of shrew-rats (*Rhynchomys*: Muridae: Rodentia) from Luzon Island, Philippines

Eric A. Rickart,* Danilo S. Balete,† Robert M. Timm, Phillip A. Alviola, Jacob A. Esselstyn, and Lawrence R. Heaney

Natural History Museum of Utah, University of Utah, Salt Lake City, UT 84108, USA (EAR)
Field Museum of Natural History, 1400 S Lake Shore Drive, Chicago, IL 60605, USA (DSB, LRH)
Department of Ecology and Evolutionary Biology, University of Kansas, Lawrence, KS 66045, USA (RMT)
Institute of Biological Sciences, University of the Philippines, Los Baños, Laguna 4031, Philippines (PAA)
Museum of Natural Science and Department of Biological Sciences, Louisiana State University, Baton Rouge, LA 70803, USA (JAE)

* *Correspondent: rickart@umnh.utah.edu*
† *Deceased 1 July 2017.*

The murine genus *Rhynchomys* includes the large-bodied Philippine "shrew-rats," highly specialized members of the vermivorous clade of Philippine murids. Four species are recognized, all of which are endemic to Luzon Island: *R. soricoides* from mountains within the Central Cordillera, *R. isarogensis* from Mt. Isarog on the Bicol Peninsula, *R. banahao* from Mt. Banahaw in south-central Luzon, and *R. tapulao* from Mt. Tapulao in the Zambales Mountains. Field surveys in 2006 and 2008 revealed two additional populations of *Rhynchomys*, one from Mt. Labo (1,544 m), a dormant stratovolcano at the base of the Bicol Peninsula, the other from Mt. Mingan (1,901 m), the highest peak in the central Sierra Madre of east-central Luzon. Assessment of external and craniodental features of available specimens from throughout Luzon support our description of the populations on Mt. Labo and Mt. Mingan as new species. All species of *Rhynchomys* are restricted to high-elevation, montane, and mossy forest habitats, separated by intervening lowlands. These discoveries highlight the importance of isolated highland areas in the historical diversification of Southeast Asian murines, and as current centers of endemism.

Key words: biogeography, Chrotomyini, conservation, distribution, ecology, morphology, oceanic islands, systematics

The family Muridae is the most diverse and speciose family of mammals, with some 157 genera and more than 834 species currently recognized (Burgin et al. 2018). Much of this diversity resulted from ancient radiations on separate continents and island groups (Steppan et al. 2004; Musser and Carleton 2005; Jansa et al. 2006; Rowe et al. 2008, 2016). One of the most remarkable radiations produced the endemic Philippine shrew-rats comprising the genera *Archboldomys* Musser, 1982; *Chrotomys* Thomas, 1895; *Rhynchomys* Thomas, 1895; and *Soricomys* Balete et al., 2012, and together include 13 described species having specialized diets consisting of earthworms and soft-bodied arthropods (Heaney et al. 2016). Together with their sister group, the omnivorous forest mice (*Apomys*), the shrew-rats comprise the tribe Chrotomyini (Rowsey et al. 2018). The chrotomyines are postulated to represent the descendants of a very early colonist of the oceanic Philippines (Musser and Heaney 1992; Jansa et al. 2006), with a median estimate of 8.4 ± 0.9 mya (Rowsey et al. 2018). The closest relatives of Chrotomyini comprise a monophyletic group of morphologically disparate murines of Australia and New Guinea (Rowe et al. 2008, 2016; Schenk et al. 2013).

Morphologically, *Rhynchomys* is the most distinctive of the chrotomyine genera. There are four described species: *R. banahao* Balete et al., 2007; *R. isarogensis* Musser and Freeman, 1981; *R. soricoides* Thomas, 1895; and *R. tapulao* Balete et al., 2007, all from areas of high-elevation forest on Luzon (Thomas 1895; Musser and Freeman 1981; Balete et al. 2007). *Rhynchomys* is characterized by an extremely long rostrum, long, slender mandibles bearing thin, saber-like lower incisors, greatly reduced molars, and a suite of other characters that reflect specialized diet and behavior (Heaney et al. 2016). The only murine that remotely resembles *Rhynchomys* is the

Sulawesi endemic *Paucidentomys* Esselstyn, Achmadi, and Rowe, 2012, an independent derivation of this distinctive vermivore morphology (Esselstyn et al. 2012; Rowe et al. 2016).

Oldfield Thomas (1895, 1898) described *Rhynchomys* as a monotypic genus and named *R. soricoides* as its type, based on five specimens collected by John Whitehead in 1895 on Mt. Data, in the Central Cordillera of northern Luzon (Fig. 1). Nearly a century later, Musser and Freeman (1981) described the second known species, *R. isarogensis*, based upon a single specimen from Mt. Isarog, a dormant stratovolcano on the Bicol Peninsula of southeastern Luzon (Fig. 1). Subsequent fieldwork (1988–1994) on Mt. Isarog produced additional examples of this species (Rickart et al. 1991; Heaney et al. 1999). From 2001, fieldwork throughout Luzon has greatly increased the number of specimens of *Rhynchomys*, resulting in the discovery and description of two additional species: *R. banahao* from Mt. Banahaw in south-central Luzon, and *R. tapulao* from Mt. Tapulao (= Mt. High Peak) in the Zambales Mountains of west-central Luzon (Balete et al. 2007).

Recent field surveys on Mt. Labo (1,544 m), a dormant andesitic stratovolcano at the base of the Bicol Peninsula about 60 km northwest of Mt. Isarog, and Mt. Mingan (1,901 m) in the central Sierra Madre range of east-central Luzon (Fig. 1), produced additional specimens of *Rhynchomys.* These differ from the four previously known species in body size and proportions, color, and features of the skull and dentition. Herein, we describe the specimens from Mt. Labo and Mt. Mingan as new species, summarize what we know of their natural history and conservation status, and discuss their significance to the biogeography of Luzon.

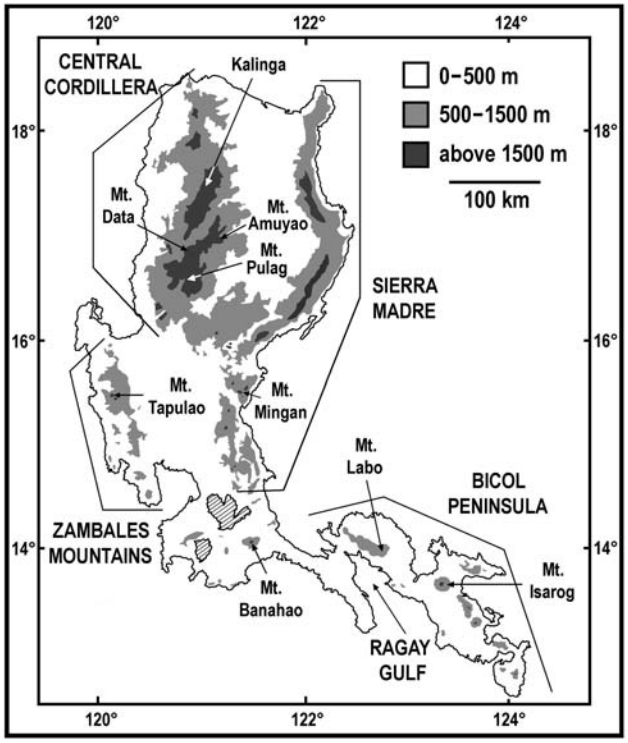

Fig. 1.—Map of Luzon Island, Philippines, showing location of places mentioned in the text.

Materials and Methods

Specimens examined in this study (Appendix I) are deposited at the Field Museum of Natural History (FMNH), University of Kansas Natural History Museum (KU), and the United States National Museum of Natural History, Smithsonian Institution (USNM). We assigned specimens to age categories based on relative body size, reproductive condition, relative closure of cranial sutures, and degree of molar tooth wear (Musser and Heaney 1992). Terms for external features are from Brown (1971) and Brown and Yalden (1973), and those for cranial and dental features follow Musser and Heaney (1992). Scanning electron micrographs of teeth are from uncoated specimens.

Measurements (in millimeters) of total length (TOT), length of tail (LT), length of hind foot including claws (LHF), length of ear from notch (LE), and weight in grams (WT) recorded from fresh specimens prior to preservation were taken from field catalogs of the authors and their associates located at FMNH, KU, and USNM. The length of the head plus body (LHB) was determined by subtracting LT from TOT. Length of over-fur (LOF) was measured mid-dorsally, and the number of tail scale rings per centimeter (TSR) was counted at a point on the dorsal surface of the tail one-third of the length from the base (Musser and Heaney 1992).

Twenty-seven cranial, mandibular, and dental measurements were taken from 38 adult specimens of *Rhynchomys*. Most measurements are defined and illustrated in Musser and Heaney (1992) and others are defined here: greatest length of skull (GLS), least interorbital breadth (IB), zygomatic breadth (ZB), breadth of braincase (BBC), height of braincase (HBC), length of nasal bones (LN), length of rostrum (LR), greatest posterior breadth of rostrum across nasolacrimal capsules (PBR), least medial breadth of rostrum near the premaxillary–maxillary suture (MBR), greatest anterior breadth of rostrum across the upper incisor capsules (ABR), breadth of zygomatic plate (BZP), length of diastema (LD), palatal length (PL), postpalatal length (PPL), length of incisive foramen (LIF), breadth across incisive foramina (BIF), distance from posterior edge of incisive foramina to anterior margin of M1 (IF–M1), length of palatal bridge (LPB), palatal breadth at M1 (PBM1), breadth of mesopterygoid fossa (BMF), length of auditory bulla (LB), height of auditory bulla (HB), breadth across incisor tips (BIT), crown length of maxillary molar toothrow (LM1–2), crown breadth of M1 (BM1), length of mandible plus lower incisor (LMI), and posterior height of mandible (HM). All cranial measurements were taken by Rickart using dial calipers and recorded to the nearest 0.1 mm. Dimensions of the baculum were measured using a dissecting microscope with a calibrated ocular micrometer and recorded to the nearest 0.05 mm.

We used Microsoft Excel for Windows (version 2016) to calculate descriptive statistics (mean, *SD*, and range). We used the Mann–Whitney *U*-test to assess sample differences in external and cranial measurement. Given the small sample sizes, statistical assessment of sexual dimorphism was not feasible, and we pooled measurements of males and females in our analyses of variation among groups. We assessed quantitative phenetic variation in craniodental morphology through principal

component analysis (PCA—using the correlation matrix) of $\log_{10}$-transformed measurements of adult specimens using SYSTAT 10 for Windows (SPSS Inc. 2000). We used a subset of cranial measurements in order to include specimens with slightly damaged skulls and to have the number of individuals exceed the number of variables in our analyses. We considered components having eigenvalues of less than 1.5 as uninterpretable. We used bivariate plots of principal component axes and raw measurement data to illustrate morphological differences among taxa.

We conducted fieldwork in accordance with all pertinent Philippine laws and regulations. Scientific study permits were granted by the Philippine Department of Environment and Natural Resources. The capture and handling of animals in the field followed guidelines established by the American Society of Mammalogists (Sikes et al. 2016).

Results

Among the sample groups of *Rhynchomys*, there are moderate differences in body size, external proportions, and craniodental measurements (Tables 1 and 2). There is no qualitatively discernable sexual dimorphism within any of the groups. We conducted a PCA on a subset of 20 craniodental measurements taken from 27 adult and young adult specimens with intact or only slightly damaged crania including *R. banahao* (n = 1), *R. isarogensis* (n = 7), *R. soricoides* (n = 7), *R. tapulao* (n = 3), and specimens from Mt. Labo (n = 6) and Mingan (n = 3). The first four components of the PCA each had eigenvalues greater than 1.5, and together accounted for 80% of the total variance (Supplementary Data SD1). Component 1 accounted for 46.6% of the variance; all of the variables had positive loadings, and more than half were of high magnitude, indicating that this axis reflected variation in size. Component 2, accounting for 15.1% of the variance, had strong positive loadings for anterior, medial, and posterior rostral breadth, and PBM1, thus separating individuals with broad rostra and palates from specimens with the opposite features. Component 3 (10.8%) separated specimens having broad interorbital regions, rostra that are broad posteriorly, and narrow palates from those having the converse. Component 4 (7%) distinguished specimens having narrow zygomatic plates and larger molars from those with the opposite features.

A bivariate plot of specimen scores on the first two principal components (Fig. 2A) reveals nearly complete separation of the geographic sample groups. *R. isarogensis* and the specimens from Mt. Labo have partially overlapping low scores on component 1 reflecting their shared smaller size compared to other groups. They likewise partially overlap on component 2 indicating similarities in shape. The remaining groups are entirely separated. Specimens of *R. soricoides* have the highest scores on the first component, reflecting their large size, and a broad range on component 2, indicating considerable intraspecific variation in shape. *R. banahao*, *R. tapulao*, and specimens from Mt. Mingan share intermediate scores on component 1, reflecting similar size, but are well separated on component 2, indicating substantial shape differences.

Table 1.—External measurements ($X \pm 1$ *SD* and ranges, in millimeters; weight in grams) and measurement ratios (expressed as percentages) of adult *Rhynchomys*. Sample sizes in parentheses. LE = length of ear from notch; LHB = length of the head plus body; LHF = length of hind foot including claws; LOF = Length of over-fur; LT = length of tail; TSR = number of tail scale rings per centimeter; WT = weight in grams.

	Rhynchomys banahao		*Rhynchomys isarogensis*		*Rhynchomys soricoides*		*Rhynchomys tapulao*		*Rhynchomys labo*			*Rhynchomys mingan*		
	Females	Males	Females	Males	Females	Males	Female	Males	Holotype	Females	Males	Holotype	Females	Males
LHB	174.0	184.0	172.8 ± 5.7	175.2 ± 6.0	193.2 ± 7.9	194.0 ± 10.7	188 (1)	170	175	175.3 ± 10.7	177.6 ± 9.2	191	187.1 ± 6.3	186.6 ± 9.2
	168–180 (2)	178–190 (2)	164–180 (10)	160–184 (18)	180–204 (13)	180–219 (18)		154–174 (2)		157–189 (8)	157–192 (14)		175–196 (10)	175–199 (8)
LT	123.5	129.0	115.3 ± 3.5	119.7 ± 3.4	146.4 ± 7.3	146.7 ± 8.2	120 (1)	127	106	103.6 ± 5.5	105.9 ± 3.1	126	126.0 ± 4.5	126.6 ± 5.2
	121–126 (2)	127–130 (2)	108–118 (10)	115–126 (18)	134–158 (13)	132–165 (18)		126–128 (2)		97–114 (8)	100–111 (14)		118–132 (10)	119–134 (8)
LHF	39.5	39.5	38.0 ± 1.1	38.4 ± 0.7	41.5 ± 1.6	41.5 ± 1.4	40 (1)	39	38	36.5 ± 1.4	37.0 ± 1.0	41	39.9 ± 0.6	40.0 ± 1.0
	39–40 (2)	39–40 (2)	37–40 (10)	37–40 (18)	39–44 (13)	39–44 (18)		38–39 (2)		35–39 (8)	36–39 (14)		39–41 (10)	36–44 (8)
LE	23.5	25 (2)	22.2 ± 0.4	22.0 ± 0.7	24.2 ± 0.9	24.8 ± 0.7	24 (1)	25 (2)	20	21.3 ± 1.0	21.4 ± 0.7	22	22.3 ± 0.8	22.3 ± 1.0
	23–24 (2)		22–23 (10)	21–23 (18)	22–25 (13)	24–26 (18)				20–23 (7)	20–22 (14)		21–24 (10)	21–24 (7)
WT	121.5	152.5	121.5 ± 9.1	124.2 ± 10.8	166.2 ± 12.7	173.1 ± 23.3	155 (1)	134.5	160	163.1 ± 17.2	155.3 ± 10.5	160	162.7 ± 16.4	161.4 ± 11.0
	108–135 (2)	150–155 (2)	110–140 (10)	110–145 (18)	150–180 (12)	140–220 (18)		129–140 (2)		138–182 (8)	134–170 (14)		132–172 (10)	148–176 (8)
LT/LHB (%)	71	70	67	68	76	76	64 (1)	75	61	59	60	66	67	68
	70–72 (2)	68–71 (2)	61–72 (10)	65–75 (18)	68–84 (13)	66–84 (18)		73–77 (2)		56–67 (8)	55–67 (14)		64–74 (10)	66–71 (8)
LHF/LHB (%)	23	21	22	22	21	21	21 (1)	23	22	21	20	21	21	21
	22–24 (2)	21–22 (2)	21–24 (10)	21–24 (18)	20–23 (13)	20–23 (18)		22–23 (2)		19–25 (8)	19–24 (14)		20–23 (10)	20–23 (8)
LOF	12 (2)	12–13 (2)	12–13 (3)	12 (1)	11–13 (9)	11–14 (14)	12 (1)	11 (2)		10–12 (5)	10–11 (11)	11	10–12 (8)	10–12 (6)
TSR	18–19 (2)	18–19 (2)	20–21 (3)	20 (1)	14–18 (9)	15–18 (14)	20 (1)	20 (2)		18–20 (5)	17–19 (11)	16	15–17 (8)	15–17 (6)

Table 2.—Cranial and dental measurements ($X \pm 1$ *SD* and ranges, in millimeters) of adult *Rhynchomys*. Sample sizes in parentheses. ABR = greatest anterior breadth of rostrum across the upper incisor capsules; BBC = breadth of braincase; BIF = breadth across incisive foramina; BIT = breadth across incisor tips; BM1 = crown breadth of M1; BMF = breadth of mesopterygoid fossa; BZP = breadth of zygomatic plate; GLS = greatest length of skull; HB = height of auditory bulla; HBC = height of braincase; HM = posterior height of mandible; IB = least interorbital breadth; IF–M1 = distance from posterior edge of incisive foramina to anterior margin of M1; LB = length of auditory bulla; LD = length of diastema; LIF = length of incisive foramen; LM1–2 = crown length of maxillary molar toothrow; LMI = length of mandible plus lower incisor; LN = length of nasal bones; LPB = length of palatal bridge; LR = length of rostrum; MBR = least medial breadth of rostrum near the premaxillary–maxillary suture; PBM1 = palatal breadth at M1; PBR = greatest posterior breadth of rostrum across nasolacrimal capsules; PL = palatal length; PPL = post-palatal length; ZB = zygomatic breadth.

	Rhynchomys banahao	*Rhynchomys isarogensis*		*Rhynchomys soricoides*		*Rhynchomys tapulao*		*Rhynchomys labo*			*Rhynchomys mingan*	
	Males	Females	Males	Females	Males	Female	Males	Holotype	Females	Males	Holotype	Males
GLS	45.6 (1)	43.6 ± 0.7 42.8–44.4 (4)	44.1 ± 0.6 43.4–44.7 (4)	47.8 ± 1.9 45.4–49.6 (4)	47.5 ± 3.3 42.7–50.0 (4)	46.6 (1)	45.1 45.0–45.1 (2)	43.3	43.2 (1)	43.2 ± 0.6 42.5–44.0 (5)	46.7	46.4 ± 0.2 46.3–46.7 (3)
IB	7.1 (1)	7.1 ± 0.1 6.9–7.1 (4)	7.0 ± 0.2 6.7–7.1 (4)	6.8 ± 0.7 6.5–7.0 (5)	6.9 ± 0.2 6.7–7.1 (4)	6.7 (1)	6.8 (2)	6.7	6.6 6.5–6.7 (2)	6.6 ± 0.1 6.5–6.7 (5)	7.1	7.1 ± 0.2 7.0–7.3 (3)
ZB	17.4 (1)	16.7 ± 0.6 16.1–17.5 (4)	16.9 ± 0.5 16.3–17.3 (4)	17.5 ± 0.5 16.9–18.2 (5)	17.7 ± 0.5 17.1–18.1 (3)	16.6 (1)	16.4 16.3–16.4 (2)	17.2	17.3 17.2–17.3 (2)	17.1 ± 0.3 16.7–17.5 (6)	17.2	17.4 ± 0.4 17.1–17.8 (3)
BBC	16.8 (1)	15.9 ± 0.3 15.6–16.2 (4)	16.2 ± 0.6 15.6–16.7 (4)	16.5 ± 0.2 16.2–16.7 (5)	16.8 ± 0.4 16.4–17.4 (4)	16.2 (1)	16.2 16.1–16.3 (2)	16.2	16.1 (1)	16.1 ± 0.2 15.8–16.3 (6)	16.6	16.6 ± 0.1 16.6–16.7 (3)
HBC	12.4 (1)	12.1 ± 0.1 12.1–12.2 (4)	12.4 (4)	12.6 ± 0.3 12.3–13.0 (5)	12.8 ± 0.3 12.7–13.2 (4)		12.8 12.6–12.9 (2)	12.2	12.4 12.3–12.5 (2)	12.4 ± 0.3 12.0–12.9 (6)	13.0	12.9 12.8–13.0 (2)
LN	17.4 17.2–17.5 (2)	17.0 ± 0.4 16.7–17.6 (4)	17.0 ± 0.8 16.7–18.0 (4)	19.4 ± 0.7 18.6–20.0 (4)	19.5 ± 0.5 19.0–20.1 (4)	17.8 (1)	17.8 17.7–17.9 (2)	17.4	17.5 (1)	17.6 ± 0.3 17.1–17.9 (5)	18.2	18.7 ± 0.5 18.2–19.1 (3)
LR	19.4 19.2–19.6 (2)	18.0 ± 0.3 17.8–18.3 (4)	18.0 ± 0.5 17.4–18.5 (4)	20.7 ± 0.8 19.7–21.4 (4)	21.0 ± 0.9 20.1–22.0 (4)	20.1 (1)	19.3 19.0–19.6 (2)	18.0	17.8 (1)	18.2 ± 0.2 18.0–18.5 (5)	19.6	20.0 ± 0.5 19.6–20.5 (3)
PBR	7.5 7.3–7.7 (2)	7.4 ± 0.2 7.2–7.5 (4)	7.5 ± 0.3 7.2–7.8 (4)	7.2 ± 0.3 6.8–7.6 (5)	7.3 ± 0.3 7.0–7.6 (5)	7.1 (1)	7.2 7.1–7.3 (2)	7.2	7.1 7.0–7.2 (2)	7.2 ± 0.1 7.0–7.3 (5)	7.3	7.3 ± 0.1 7.3–7.4 (3)
MBR	4.3 4.2– 4.4 (2)	4.1 ± 0.1 4.0–4.2 (4)	4.0 ± 0.1 3.9–4.1 (3)	3.9 ± 0.1 3.7–4.0 (5)	3.9 ± 0.2 3.7–4.1 (4)	3.9 (1)	4.0 (2)	4.0	4.0 3.9–4.0 (2)	4.1 ± 0.1 4.0–4.1 (5)	4.3	4.3 ± 0.1 4.2–4.3 (3)
ABR	4.6 4.5– 4.6 (2)	4.2 ± 0.1 4.1–4.3 (4)	4.1 ± 0.1 4.0–4.2 (3)	4.2 ± 0.1 4.1–4.4 (5)	4.2 ± 0.2 4.0–4.3 (4)	4.3 (1)	4.3 (2)	4.2	4.3 4.2–4.3 (2)	4.3 ± 0.1 4.2–4.5 (5)	4.3	4.3 ± 0.1 4.3–4.4 (3)
BZP	2.0 (2)	2.0 ± 0.2 1.7–2.2 (4)	2.0 ± 0.2 1.8–2.2 (4)	2.1 ± 0.2 1.9–2.4 (5)	2.1 ± 0.2 1.9–2.4 (4)	1.8 (1)	1.7 1.6–1.8 (2)	1.9	2.2 2.1–2.2 (2)	2.1 ± 0.1 1.9–2.2 (6)	2.0	2.0 ± 0.1 2.0–2.1 (3)
LD	14.1 14.0–14.2 (2)	13.3 ± 0.3 12.9–13.5 (4)	13.0 ± 0.4 12.5–13.4 (4)	15.1 ± 0.9 14.0–16.0 (5)	15.8 ± 0.5 15.1–16.2 (4)	14.2 (1)	14.2 14.1–14.2 (2)	12.9	12.9 12.6–13.1 (2)	12.8 ± 0.4 12.4–13.3 (5)	14.2	14.4 ± 0.3 14.2–14.7 (3)
PL	21.9 21.7–22.1 (2)	20.4 ± 0.7 19.8–21.3 (4)	20.4 ± 0.7 19.6–21.2 (4)	22.9 ± 0.5 22.0–24.8 (5)	24.1 ± 0.5 23.5–24.8 (4)	20.8 (1)	20.8 20.6–20.9 (2)	19.8	19.3 19.0–19.5 (2)	19.4 ± 0.4 19.0–19.9 (5)	23	23.0 ± 0.5 22.5–23.4 (3)
PPL	15.1 (1)	15.0 ± 0.3 14.6–15.2 (4)	14.9 ± 0.2 14.6–15.1 (4)	16.3 ± 0.5 15.7–16.8 (4)	16.3 ± 0.1 16.2–16.4 (4)		15.7 15.5–15.9 (2)	16.0	15.1 15.0–15.1 (2)	15.8 ± 0.2 15.5–16.0 (5)	15.7	16.0 15.7–16.2 (2)
LIF	6.3 6.1–6.4 (2)	5.8 ± 0.4 5.2–6.2 (4)	6.0 ± 0.2 5.7–6.3 (4)	7.1 ± 0.1 7.0–7.2 (5)	7.3 ± 0.4 6.8–7.8 (4)	6.7 (2)	6.5 6.2–6.8 (2)	6.1	6.1 (2)	6.1 ± 0.1 6.0–6.2 (5)	6.4	6.5 ± 0.1 6.4–6.5 (3)
BIF	2.0 1.9–2.0 (2)	1.8 ± 0.2 1.7–2.0 (4)	1.9 ± 0.1 1.7–2.0 (4)	1.9 ± 0.2 1.7–2.1 (5)	2.0 ± 0.1 1.9–2.1 (4)	2.0 (1)	2.0 1.9–2.0 (2)	1.8	1.9 1.8–2.0 (2)	1.9 ± 0.1 1.8–2.0 (5)	2.0	1.9 ± 0.1 1.9–2.0 (3)
IF–M1	5.3 5.2–5.3 (2)	5.4 ± 0.2 5.2–5.6 (4)	5.3 ± 0.1 5.2–5.3 (4)	5.7 ± 0.4 5.2–6.2 (5)	5.8 ± 0.3 5.6–6.2 (4)	5.4 (1)	5.7 5.5–5.8 (2)	5.0	4.9 4.7–5.0 (2)	4.8 ± 0.2 4.5–5.0 (5)	5.3	5.0 ± 0.3 4.8–5.3 (3)
LPB	13.8 (2)	12.9 ± 0.4 12.3–13.1 (4)	13.1 ± 0.3 12.9–13.4 (4)	14.1 ± 0.9 12.8–15.2 (5)	14.2 ± 0.6 13.7–15.0 (4)	13.1 (1)	12.4 (2) 12.1–12.6 (2)	11.5	11.7 11.6–11.8 (2)	11.6 ± 0.2 11.3–11.9 (5)	13.5	13.9 ± 0.4 13.5–14.2 (3)
PBM1	7.1 7.0–7.1 (2)	6.4 ± 0.1 6.3–6.5 (4)	6.7 ± 0.2 6.5–6.9 (4)	6.8 ± 0.3 6.4–7.2 (5)	6.9 ± 0.3 6.6–7.2 (4)	6.7 (1)	6.6 (2)	7.0	6.6 6.4–6.8 (2)	7.0 ± 0.2 6.7–7.2 (5)	6.8	7.0 ± 0.2 6.8–7.1 (3)
BMF	2.0 (2)	2.1 ± 0.1 2.0–2.2 (4)	2.1 ± 0.2 2.0–2.4 (4)	2.0 ± 0.2 1.6–2.3 (5)	1.8 ± 0.3 1.4–2.1 (4)	2.2 (1)	2.2 2.0–2.3 (2)	2.1	2.1 2.0–2.2 (2)	2.1 ± 0.2 2.0–2.5 (5)	2.2	1.9 ± 0.3 1.6–2.2 (3)

Table 2.—*Continued*

	Rhynchomys banahao	*Rhynchomys isarogensis*		*Rhynchomys soricoides*		*Rhynchomys tapulao*		*Rhynchomys labo*		*Rhynchomys mingan*	
	Males	Females	Males	Females	Males	Female	Males	Holotype	Females	Males	Holotype	Males
LB	5.3 (1)	5.1 ± 0.2	5.3 ± 0.1	5.4 ± 0.3	5.4 ± 0.2	5.6 (1)	5.4	5.0	4.6	4.9 ± 0.2	4.9	5.1 ± 0.2
		4.9–5.4 (4)	5.1–5.4 (4)	5.1–5.7 (5)	5.2–5.7 (4)		5.2–5.5 (2)		4.4–4.7 (2)	4.5–5.1 (6)		4.9–5.3 (3)
HB	5.2 (1)	4.9 ± 0.1	4.9 ± 0.1	5.0 ± 0.2	5.1 ± 0.2	5.4 (1)	5.4	4.7	4.9	4.7 ± 0.2	4.9	5.1 ± 0.2
		4.8–5.1 (4)	4.8–5.1 (4)	4.8–5.2 (5)	4.9–5.2 (4)		5.2–5.5 (2)		4.6–5.2 (2)	4.5–4.9 (6)		4.9–5.2 (3)
BIT	1.6	1.4 ± 0.1	1.4 ± 0.1	1.5 ± 0.1	1.6 ± 0.1	1.6 (1)	1.5 (2)	1.5	1.5 (2)	1.5 ± 0.1	1.4	1.5 ± 0.1
	1.5–1.7 (2)	1.3–1.5 (4)	1.3–1.5 (4)	1.5–1.6 (4)	1.5–1.7 (4)					1.5–1.6 (5)		1.4–1.6 (3)
LM1–2	2.4	2.2 ± 0.1	2.4 ± 0.2	2.5 ± 0.2	2.3 ± 0.1	2.2 (1)	2.5 (2)	2.3	2.2	2.3 ± 0.1	2.6	2.5 ± 0.1
	2.3–2.5 (2)	2.1–2.3 (4)	2.2–2.6 (4)	2.3–2.8 (5)	2.2–2.4 (3)				2.1–2.2 (2)	2.2–2.4 (5)		2.4–2.6 (3)
BM1	1.0 (2)	1.0 ± 0.1	1.0 ± 0.1	1.0 ± 0.1	1.0 ± 0.1	0.9 (1)	1.0 (2)	1.0	1.0 (2)	1.0 (5)	1.0	1.0 (3)
		0.9–1.0 (4)	0.9–1.0 (4)	0.9–1.1 (5)	0.9–1.0 (3)							
LMI	31.3	30.4 ± 0.8	30.8 ± 0.7	33.2 ± 0.9	34.8 ± 0.7	31.9 (1)	31.2	30.3	29.0	29.8 ± 0.6	32.6	32.4 ± 0.2
	31.0–31.5 (2)	29.5–31.4 (4)	30.1–31.7 (4)	32.1–34.2 (4)	34.2–35.6 (3)		31.0–31.3		28.7–29.2 (2)	29.0–30.4 (6)		32.2–32.6 (3)
HM	7.6	7.7 ± 0.2	7.8 ± 0.1	8.2 ± 0.3	8.0 ± 0.5	7.4 (1)	7.2 (2)	7.1	7.2	7.3 ± 0.3	8.1	7.6 ± 0.4
	7.2–7.9 (2)	7.5–7.9 (4)	7.6–7.9 (4)	7.8–8.6 (5)	7.5–8.4 (3)		7.1–7.3 (2)		7.0–7.3 (2)	7.0–7.7 (6)		7.3–8.1 (3)

To assess the differences among the groups from southern Luzon in more detail, we conducted a separate PCA using a subset of 12 cranial measurements from specimens of *R. banahao* (n = 1), *R. isarogensis* (n = 7), and from Mt. Labo (n = 6). In this analysis, principal components 1 and 2 had eigenvalues greater than 1.5, and collectively accounted for 70% of the total variance (Supplementary Data SD2). High-magnitude variable loadings on the first component (41.9% of the variance) reflect the substantial size range across these groups. On component 2, accounting for 28.2% of the variance, half of the variables had high-magnitude loadings reflecting important shape differences among the groups. This component distinguished individuals having narrow interorbital regions, broad braincases, wide anterior rostral breadth, broad zygomatic plates, long incisive foramina, and short, broad palates from those specimens with the opposite features. Components 3 and 4 had eigenvalues of less than 1.5 and therefore were considered uninterpretable.

In a plot of specimen scores on the first two components (Fig. 2B), the three groups are completely separated. On the first component, primarily reflecting size, specimens from Mt. Labo have the lowest scores, the single specimen of *R. banahao* has the highest, and *R isarogensis* are intermediate. On component 2, reflecting primarily shape differences, *R. isarogensis* has a broad range of low to intermediate scores; specimens from Mt. Labo are entirely separate with higher scores, and the single specimen of *R. banahao* is intermediate.

We conducted a third PCA to further assess differences among the three groups from northern and central Luzon, *R. soricoides* (n = 10), *R. tapulao* (n = 3), and specimens from Mt. Mingan (n = 3), using the same subset of 12 cranial measurements used in the analysis of the southern group (Supplementary Data SD3). The first two components had eigenvalues greater than 1.5 and together accounted for nearly 68% of the variance. Many characters had high-magnitude loadings on component 1, which accounted for 45.1% of the variance, principally reflecting size differences. Component 2, accounting for 22.9% of the variance, separated individuals with broad interorbital regions, broad rostra, short diastemas, and small auditory bullae from those with the opposite features. With eigenvalues less than 1.5, components 3 and 4 were not interpretable.

A bivariate plot of specimen scores on the first two components (Fig. 2C) shows complete separation of the three groups. Within *R. soricoides*, there is substantial variation on both components; the largest individuals are those from Mt. Pulog and Mt. Data, the smallest from Mt. Amuyao, and those from Kalinga Province are intermediate in size. The Pulog and Mt. Data specimens, along with one individual from Kalinga Province, have intermediate scores on the second component, whereas two other individuals from Kalinga and the single specimen from Mt. Amuyao have negative scores on this axis. This distribution of scores reveals both geographic and non-geographic size and shape variation within the broad sample of *R. soricoides.* In this analysis, specimens of *R. tapulao* are the smallest individuals, as reflected in their low scores on component 1; on component 2, they share intermediate scores with some *R. soricoides* specimens. Specimens from Mt. Mingan have intermediate scores on component 1, consistent with their relative size, and have the highest

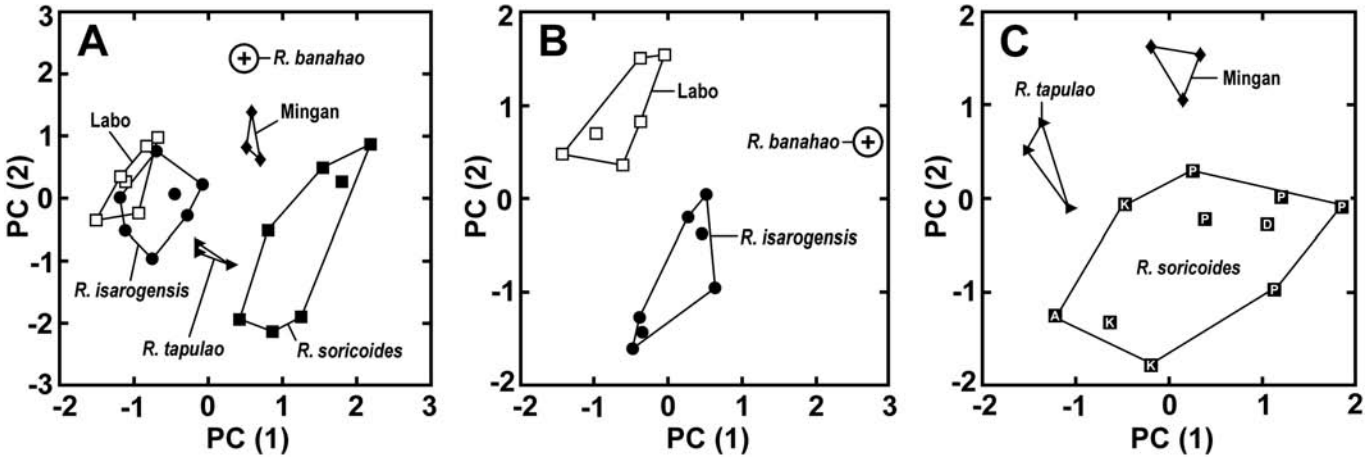

Fig. 2.—Results of principal components analyses of cranial and dental measurements of *Rhynchomys* (see text and Table 1). Projections of individual specimen scores on components 1 and 2 for (A) analysis including all six groups, (B) analysis for three groups from southern Luzon, and (C) analysis for three groups from central and northern Luzon.

scores on component 2, revealing substantial shape differences compared to the other species.

These results, together with additional comparisons made below, reaffirm the recognition of the four previously recognized species: *R. soricoides* from the Central Cordillera of northern Luzon, *R. tapulao* from the Zambales Mountains in west-central Luzon, *R. banahao* from Mt. Banahaw in south-central Luzon, and *R. isarogensis* from Mt. Isarog in the central Bicol Peninsula in southeastern Luzon. Results also support the recognition of two additional species, one from Mt. Mingan in the central Sierra Madre, east-central Luzon, and the other from Mt. Labo in the northern portion of the Bicol Peninsula; these we describe in the following accounts.

Rhynchomys labo, new species

Labo shrew-rat

Figs. 2–6 and 8, Tables 1 and 2

Rhynchomys sp.: Balete, Heaney, Alviola, and Rickart, 2013a:71.

Rhynchomys isarogensis: Heaney, Balete, and Rickart, 2016:160.

Holotype.—KU 165952, adult male trapped on 28 June 2008 by Jacob A. Esselstyn (field number: JAE 2196); fixed in formaldehyde solution, preserved in 70% ethanol with the skull removed and cleaned. Prior to fixation, a sample of muscle tissue was preserved in 95% ethanol. The left occipital region of the skull is slightly damaged, but otherwise all parts of the holotype are in excellent condition. The specimen, now located at the University of Kansas, is to be deposited at the Philippine National Museum of Natural History, Manila, Republic of the Philippines.

Type locality.—Mt. Labo, Barangay Tulay na Lupa, Labo Municipality, Camarines Norte Province, Luzon Island, Republic of the Philippines, 1,250 m elevation, 14.0235°N, 122.7873°E (Fig. 1; Balete et al. 2013a, figure 6A).

Paratypes.—In addition to the holotype, there are 21 specimens of *Rhynchomys labo* from localities on the northern slope of Mt. Labo. Three additional males and two females were collected at the type locality between 28 June and 1 July 2008 (KU 165951, 165953–165956). Four males and four females were collected between 3 and 6 May 2006 at 0.6 km N, 0.5 km W east peak of Mt. Labo, elevation 1,335 m, 14.02301°N, 122.78777°E (FMNH 189832–189837, 189870, 189871), and six males and two females were collected between 6 and 10 May 2006 at 0.25 km N, 0.25 km W east peak of Mt Labo, elevation 1,413 m, 14.01883°N, 122.78970°E (FMNH 189838–189844, 189872). All specimens were initially fixed in formaldehyde solution and preserved in 70% ethanol. The skulls of eight specimens were later removed and cleaned, and one male was later prepared as a study skin with a cleaned skull and baculum. Half of the paratypes, now located at either the Field Museum or the University of Kansas, are to be deposited at the Philippine National Museum of Natural History.

Distribution.—Known only from forested areas on the north slope of Mt. Labo between 1,250 and 1,413 m elevation.

Etymology.—The new species is named for Mt. Labo, where the specimens originated. The specific epithet is used as a noun in apposition. We propose "Labo shrew-rat" as the English common name.

Nomenclatural statement.—A Life Science Identifier (LSID) number was obtained for the new species (*R. labo*): urn:lsid:zoobank.org:act:ED88CCD7-D1C3-46FF-8705-76F332165A76.

Diagnosis.—*R. labo* is distinguished from other members of the genus by the following combination of traits (with contrasting characters of congeners in parentheses): dorsal pelage dark grayish brown, sharply delineated from pure white venter (dorsum and venter less sharply delineated and venter darker, or dorsum golden brown and underparts white or pale gray); forefoot unpigmented dorsally, sharply delineated from dark gray wrist (variable amount of dark hair on dorsal surface of foot, less contrast with wrist color); tail short, both absolutely and relative to LHB (tail longer); anterior tips of nasals strongly tapered to a narrow point (anterior tips broadly rounded); narrow interorbital breadth (interorbital breadth greater); auditory bullae small (bullae larger); presence of a mastoid foramen

or pit (absent in others except *R. banahao*). *R. labo* is most similar to *R. isarogensis*, which is geographically the nearest species (Fig. 1). Accordingly, comparisons between these two species are emphasized in the following section.

Description and comparisons.—R. labo (Fig. 3) is a medium-sized murid, similar in general body form to other members of the genus, but displaying differences in body size, relative proportions of the limbs and tail, pelage color, and craniodental features (Tables 1 and 2; Figs. 4, 6–8, and 10). Compared to *R. isarogensis*, *R. labo* has similar head plus body length (Mann–Whitney *U*-test: $z = -1.62$, $n_1 = 30$, $n_2 = 22$, $P = 0.11$), but substantially greater body weight ($z = 5.68$, $n_1 = 30$, $n_2 = 22$, $P < 0.001$), indicating a more robust build. Dorsal pelage of *R. labo* is dense, and slightly shorter than that of congeners. The overall dorsal coloration is dark brown similar to *R. soricoides* and the new species from Mt. Mingan, slightly darker than *R. tapulao* and *R. isarogensis*, and paler than *R. banahao*. As in congeners, individual dorsal hairs are a mix of some that are tricolored (medium gray for basal two-thirds, golden brown with black tips for the distal one-third), or bicolored (gray for basal two-thirds, black for the distal third); overall dorsal color variation is due to the proportion of the two types. Length of the mid-dorsal overfur is similar in *R. labo* and *R. isarogensis*. From the throat to the inguinal region, the venter of *R. labo* is entirely white (individual hairs unpigmented from base to tip), grading to light gray on the upper throat, chin, and the inner thighs (where hairs are gray basally with white tips). The white venter is strongly delineated from the dark dorsum, with only a very narrow lateral zone of gray hairs in between. The dark brownish gray of the dorsum extends down onto the side of the head, upper arms, and outer thighs. The strong contrast between the dorsum and venter is similar to that of *R. tapulao*, in which the venter is either pure white or white with patches of gray and contrasts sharply with the bright, golden-brown dorsum. In *R. isarogensis* and the other species, the venter is gray (sometimes with patches of white hairs) and there is less contrast between ventral and dorsal pelage.

As in congeners, the lips and rhinarium of *R. labo* are unpigmented, the eyelids are thinly lined in black, and there is a narrow pale eye ring. The dark brown mystacial vibrissae are long (the longest more than 50 mm) and extend beyond the ears; those closer to the end of the snout are shorter and paler. Less conspicuous vibrissae are located behind the eyes (genal), under the lower jaw (interramal), and under the forearm (antebrachial—Brown and Yalden 1973). The ears are dark gray and covered with short black hairs, similar in color to *R. soricoides* and *R. tapulao*, darker than those of *R. isarogensis*, and paler than those of *R. banahao*. Average ear length of *R. labo* is shorter than in other species (Table 1), and differs significantly from *R. isarogensis* ($z = 2.69$, $n_1 = 30$, $n_2 = 21$, $P < 0.01$).

The forefeet of *R. labo* are like those of the other species; large with strong digits armed with long pale claws except for the pollex that bears a short nail. Skin of the dorsal surface of the manus is unpigmented as in other species except *R. banahao*, in which it is pale gray. Scattered hairs over the entire dorsal surface are unpigmented. In the other species, hairs are darkly pigmented (*R. banahao*) or mostly unpigmented with at least some pigmented hairs extending from the wrist over the dorsolateral surface of the manus to the base of the digits (all others). As in congeners, the palmar surface is naked, unpigmented, and has three small interdigital and two larger metacarpal pads.

The hind feet of *R. labo* are, on average, shorter than those of congeners (Table 1), and are significantly shorter than those of *R. isarogensis* both absolutely ($z = 3.98$, $n_1 = 30$, $n_2 = 22$, $P < 0.001$) and relative to head plus body length (LT/LHB; $z = 3.35$, $n_1 = 30$, $n_2 = 2$s, $P < 0.001$). As in all species, the toes bear strong, pale claws. Skin of the dorsal surface of the foot is unpigmented as is the case in other species except *R. banahao*, which has dark gray pigmentation. Scattered hairs over the metatarsi and toes are mostly unpigmented except for a band of dark hairs on the lateral surface extending from the ankle to the base of the toes. The pattern of hairs on the dorsal surface of the hind foot is similar in *R. isarogensis*, *R. soricoides*, and the Mingan *Rhynchomys*; in *R. banahao*, the hairs are principally dark, whereas in *R. tapulao*, they are unpigmented. As in the other species, there are four interdigital pads, a small thenar, and elongate hypothenar. The plantar surface is naked, and from the toes to the interdigital pads unpigmented, as is the heel and a narrow, isolated band along the lateral margin between the heel and the hypothenar pad. The remainder of the plantar surface is dark gray. The pigmentation pattern is similar in *R. soricoides*, *R. tapulao*, and the Mingan *Rhynchomys*; in *R. banahao*, the entire surface is dark gray except for the tips of the toes, plantar pads, and the point of the heel, which are pale gray.

The tail of *R. labo* is shorter than in congeners (Table 1; Fig. 4A), and significantly shorter than in *R. isarogensis*, both in absolute length ($z = 5.96$, $n_1 = 30$, $n_2 = 22$, $P < 0.001$), and relative to head plus body length ($z = 5.48$, $n_1 = 30$, $n_2 = 22$, $P < 0.001$). The tail is uniformly dark in most specimens and slightly paler below in others; most individuals have a small (1–5 mm) unpigmented tip. Coloration is similar in *R. banahao*; other species have bicolored tails that are unpigmented or lightly pigmented ventrally or pigmented basally and unpigmented distally. The tail scales are larger (fewer scale rings per cm) than those of *R. isarogensis* and *R. tapulao*, but smaller than those of *R. soricoides* and *R. mingan* (Table 1). As in all *Rhynchomys*, there are three very small, stiff hairs associated with each tail scale.

The baculum of *R. labo* (Fig. 5) has an enlarged base with an acute proximal margin that is roughly triangular. The base is broad laterally and thick dorsoventrally, and accounts for about one-third the length of the bone. From the base, it tapers to form a straight (unbowed) shaft that terminates in a club-like distal tip that is slightly asymmetrical. A narrow dorsal concavity extends from the base distally halfway up the length of the bone. There is a broad concavity on the ventral surface of the base. Measurements (in millimeters) are total length 6.50, width of the base 2.25, dorsoventral thickness of the base 1.55, least width of the shaft 0.65, and width of the distal tip 1.10. The baculum of *R. labo* is relatively simple and in general resembles those of some New Guinean murids (Lidicker 1968;

Fig. 3.—*Rhynchomys labo*. Drawing by Velizar Simeonovski.

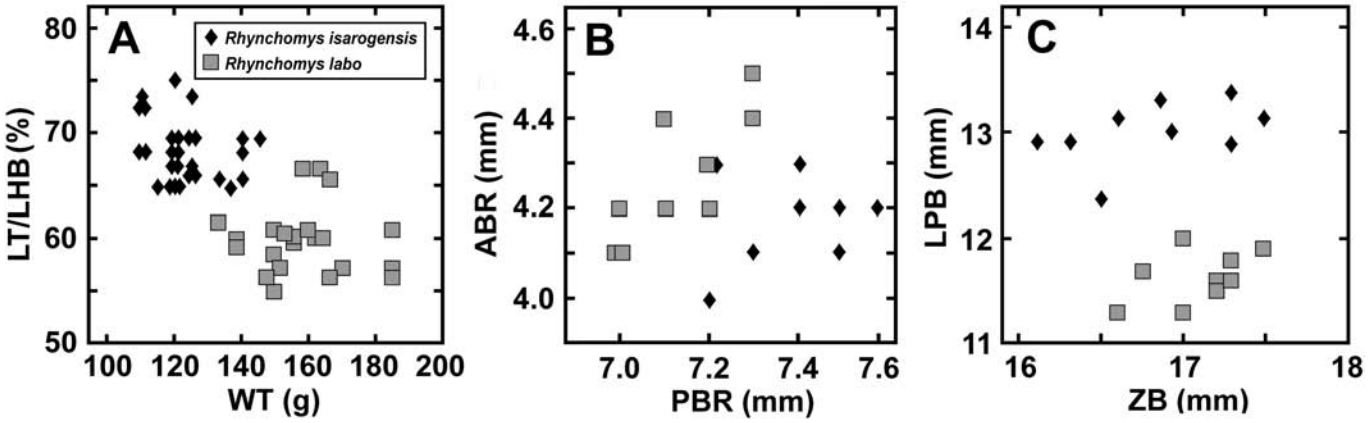

Fig. 4.—Bivariate plots of measurements and measurement ratios comparing *Rhynchomys isarogensis* and *R. labo.* A) Length of tail as a percentage of length of head and body (LT/LHB %) versus body weight (WT). B) Anterior breadth of rostrum (ABR) versus posterior breadth of rostrum (PBR). C) Length of palatal bridge (LPB) versus zygomatic breadth (ZB).

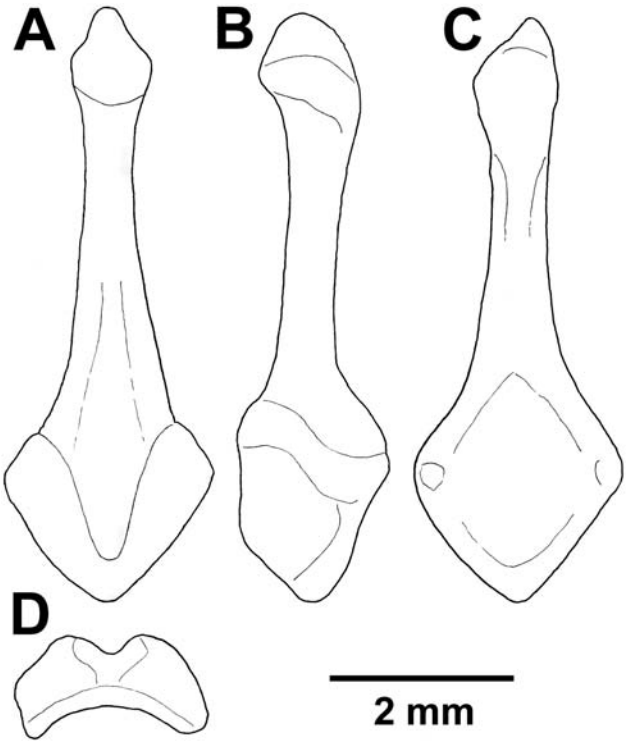

Fig. 5.—Baculum of *Rhynchomys labo*, KU 165953, paratype. A) Dorsal view. B) Lateral view (dorsal side to the left). C) Ventral view. D) Proximal end (dorsal surface upward).

Lidicker and Brylski 1987). The most notable features that distinguish it are the thickness of the base, the shape of the proximal margin, and the swollen distal end (Fig. 5; Lidicker 1968, figure 10). There is no published information on bacula of other Philippine murid rodents, and there is surprisingly little information on phallic morphology of murids in general. As in the other species of *Rhynchomys*, females have two pairs of inguinal mammae.

The general cranial morphology of *R. labo* is similar to that of congeners (Figs. 6 and 7; Balete et al. 2007, figures 4 and 5). The skull is small; length (GLS) is comparable to that of *R. isarogensis* and considerably less than in the other species (Table 2). From the dorsal perspective, the rostrum is elongate and narrow, substantially shorter than in *R. soricoides* but comparable to the other species. *R. labo* and *R. isarogensis* differ in the shape of the rostrum. The anterior breadth of the rostrum (ABR) is significantly greater in *R. labo* ($z = -1.85$, $n_1 = 8$, $n_2 = 7$, $P < 0.05$); this measurement is not significantly correlated with breadth of the upper incisors (BIT), either for individual groups or across all specimens of *Rhynchomys*. In contrast, the posterior breadth of the rostrum (PBR) is greater in *R. isarogensis* ($z = 2.54$, $n_1 = 9$, $n_2 = 7$, $P < 0.01$). A bivariate plot of these measurements reveals little overlap between the two species (Fig. 4B). Medial breadth of the rostrum (MBR) is similar in both species; however, in *R. labo*, the medial portion of the rostrum appears more constricted relative to the broader anterior and posterior portions. The nasals are long and narrow, projecting well beyond the premaxillae. The anterior nasal tips are more acutely tapered and come to a narrower point compared to those of congeners. As in the other species, the zygomatic arches are thin and strongly backswept from the maxillary roots, but posteriorly they are more robust near the squamosal roots, such that the relative difference between the ZB and the braincase breadth is greater than in the other species. The braincase is inflated and ovate in shape, tapering sharply to the interorbit that is narrower than in the other species. As in other species of *Rhynchomys*, the dorsal surface of the braincase is entirely smooth, with no hint of ridges on the supraorbital, temporal, or supraoccipital margins.

In lateral perspective (Fig. 6), the skull of *R. labo* exhibits features shared with other members of the genus. The greatly elongated rostrum is sharply tapered anteriorly, not to the extent seen in *R. soricoides* (Fig. 7), but more so than in the other taxa that have deeper rostra. The anterior premaxillary margin projects beyond the upper incisors and has a distinctive concave profile common to all *Rhynchomys*. The nasal tips extend even further beyond the premaxillae and are expanded upward as in the other species except *R. banahao*, which has a nearly straight nasal profile (Balete et al. 2007, figure 5). Posteriorly, the smooth dorsal profile is interrupted by a slight convexity over the inflated frontals, followed by a broadly curved convex profile across the top of the braincase, a flat supraoccipital profile, and abrupt transition to the occipital margin that is less inflated than in *R. isarogensis*, producing a flatter, more vertical posterior profile. As in congeners, there is little overlap between the dorsal and ventral maxillary zygomatic roots such that the zygomatic plate is strongly slanted posteriorly. The anterior margin of the plate is strongly convex as in most specimens of *R. isarogensis*, but in contrast to the other species in which the margin is less convex or nearly straight. As in congeners, the posterior portion of the squamosal root of the zygomatic arch is positioned at a point slightly above the dorsal margin of the large postglenoid vacuity. The auditory bulla is small compared to those of the other species (Table 2); length of the bulla (LB) is less than in *R. isarogensis* ($z = 2.50$, $n_1 = 9$, $n_2 = 8$, $P < 0.01$), but there is no significant difference in height (HB) indicating dissimilar shape. As in congeners, the mastoid of *R. labo* is moderately inflated. In half of the specimens examined, including the holotype (Fig. 6), there is a small foramen located near the posterior margin of the mastoid; in other specimens, instead of an open foramen, there is a closed depression or pit. *R. banahao* also has a mastoid foramen, but this character is not present in the other species (Balete et al. 2007, figure 5).

From the ventral perspective (Fig. 6), the medial constriction of the elongated rostrum is most apparent. As in the other taxa, an interpremaxillary foramen is located immediately behind the narrow incisors. In all specimens of *R. labo*, this foramen is longer than those of *R. isarogensis*, and at least as large as those of the other species. The incisive foramina are similar in shape to those of the other species. They are similar in size to those of *R. isarogensis* but smaller than in the other species (Table 2). The paired palatine grooves are prominent from the incisive foramina to the postpalatine foramina at the maxillary–palatine suture, extending to the midpoint between the postpalatine foramina and the mesopterygoid

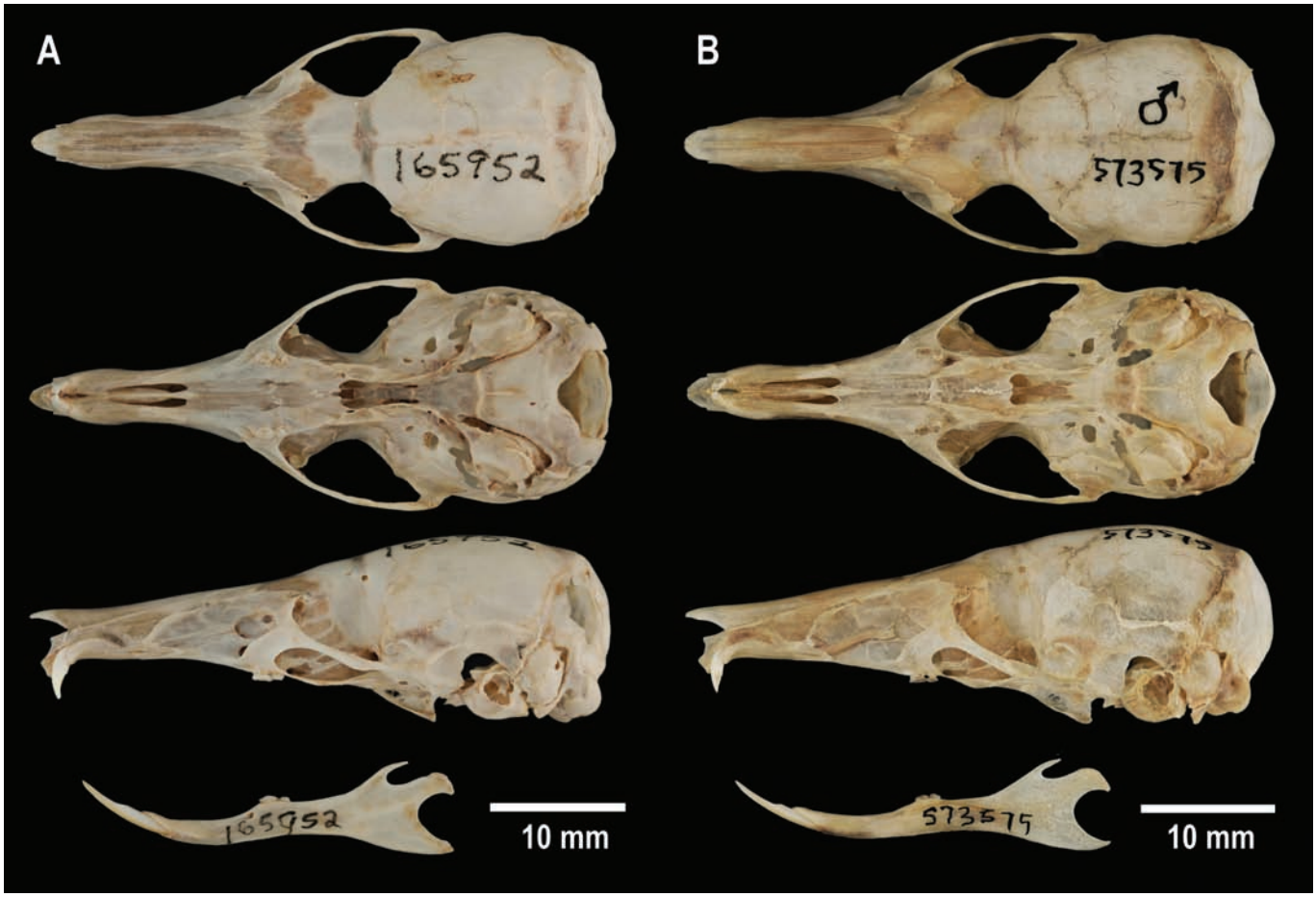

Fig. 6.—Dorsal, ventral, and lateral views of cranium and lateral view of mandible of adult *Rhynchomys*. A) *R. labo* (KU 165952, holotype). B) *R. isarogensis* (USNM 573575).

fossa. The posterior extension of the palatine grooves is more conspicuous than in *R. isarogensis.* As in other species of *Rhynchomys*, the palatine is long, narrowing posteriorly to the anterior margin of the mesopterygoid fossa. In both *R. labo* and *R. isarogensis*, LPB is less than it is in the other species (Table 2). However, the bridge is significantly shorter in *R. labo* than in *R. isarogensis* (z = 3.28, n_1 = 9, n_2 = 7, P < 0.001). A plot of LPB against ZB shows no overlap between the two species (Fig. 4C). The palate is significantly broader than in *R. isarogensis* (z = −1.91, n_1 = 9, n_2 = 7, P < 0.05). Width of the mesopterygoid fossa is similar to that of the other species except for *R. soricoides* and the Mt. Mingan *Rhynchomys*, which have narrower fossae (Table 2). The general conformation of foramina visible on the ventral surface of the skull is similar in all *Rhynchomys*. However, on the pterygoid plate, the anterior opening of the alisphenoid canal is substantially smaller in *R. labo* than it is in in the other species (Figs. 6 and 7; Musser and Heaney 1992, figure 45a). As in other *Rhynchomys*, the anterior margin of the auditory bulla is separated from the squamosal and alisphenoid by the combined postglenoid vacuity and postalar fissure. This gap, particularly the medial portion contributed by the postalar fissure, is wider in *R. labo* than it is in *R. isarogensis*, but not as wide as in *R. soricoides* or the Mt. Mingan *Rhynchomys* (Figs. 6 and 7).

In common with the other species of *Rhynchomys*, the upper incisors of *R. labo* are short, narrow, pale ivory in color, and orthodont (oriented at approximately right angles to the rostrum). The incisors are slightly broader at their tips and deeper (in lateral view) than are those of *R. isarogensis* and more similar to the other species in these dimensions (Figs. 6 and 7; Table 2). As in the other species, the anterior surface of the incisor is slightly convex in cross section such that the tips wear to a shallow crescent-shaped edge.

As in congeners, the maxillary toothrow of *R. labo* is short relative to the size of the skull, consisting of only M1 and M2, both of which are very small. Length of the toothrow and breadth of M1 are similar to those of *R. isarogensis* (Table 2). In both *R. labo* and *R. isarogensis*, a flat ridge of bone adjacent to the anterolateral margin of M1 is short, projecting only slightly beyond the anterior margin of the tooth; in the other species, this ridge forms a flat shelf extending anteriorly from M1 (Figs. 6 and 7; Balete et al. 2007, figure 4). Available skulls of *R. labo* are from specimens ranging in age from young adult to old adult (Musser and Heaney 1992) having molars with moderate to very heavy wear on the occlusal surfaces. Judging from the margins of worn cusps, the thickness of the enamel layer is comparable to that seen in other species of *Rhynchomys* (Fig. 8; Balete et al. 2007, figure 6). Molar wear may be relatively rapid in *Rhynchomys*

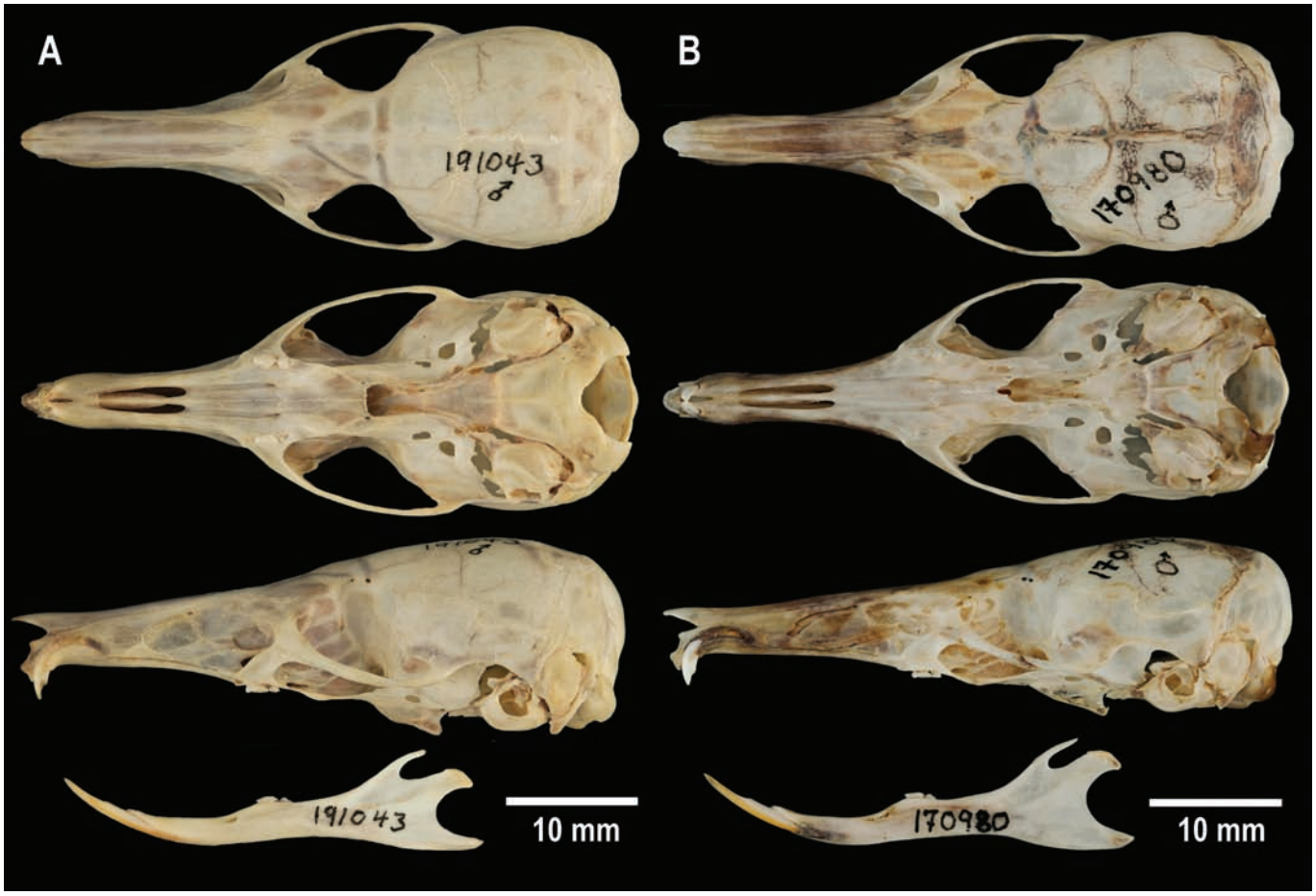

Fig. 7.—Dorsal, ventral, and lateral views of cranium and lateral view of mandible of adult *Rhynchomys*. A) *R. mingan* (FMNH 191043, holotype). B) *R. soricoides* (FMNH 170980).

given the amount of grit ingested along with earthworms. The basic cusp patterns are retained in a young adult specimen with the least-worn molars (FMNH 189833). As in the other species, M1 is narrow and tapered at each end, with three rows of cusps (Fig. 8A; Balete et al. 2007, figure 6; Musser and Heaney 1992, figure 49). The anterior group consists of a small lingual cusp (t1) and coalesced cusps t2 and t3. The second group is the most prominent and includes a large t4 isolated on the lingual margin of the tooth, together with a central t5 and labial t6 both of which are heavily worn but retain the marginal cusp outlines. The large cusp t8 dominates the posterior portion of the tooth. There is no evidence of cusp t9, which is either absent or closely coalesced with t8. As in all species of *Rhynchomys*, there is no posterior lingual cusp (t7). In all specimens of *R. labo*, lingual cusps t1 and t4 are prominent; both cusps also are present in *R. isarogensis*, but the size of t1 is variable in that species. In the other species, cusp t1 is absent. The M2 is circular in outline as in the other species and similar in size, except for in *R. banahao* in which it is considerably larger. The crown consists of two groups of cusps that retain their marginal profiles. The anterior includes t4, t5, and t6, and the posterior t8 and t9.

As in the other species, the mandible of *R. labo* is extremely long and slender with a deeply concave posterior margin (Figs. 6 and 7; Balete et al. 2007, figure 5). It is most similar in shape to that of *R. isarogensis* but smaller; those of the other species are larger (Table 2). The lower incisors of *R. labo* are similar to those of congeners; thin, broadly curved, with pale yellow enamel, and wearing to delicate, needle-like tips. Lower molars are heavily worn in the eight specimens with cleaned skulls, but the basic cusp patterns are discernable in the specimen with the least amount of wear (Fig. 8B). The crown surface of the anterior half of m1 consists of the anteroconid, metaconid, and protoconid, all of which are prominent; the posterior portion includes the entoconid, hypoconid, and a small posterior cingulum. The m2 is smaller than those of *R. banahao*, but similar in size to those of the other species. The anteroconid is small but distinct; the large protoconid dominates the labial side of the tooth and the prominent metaconid the anterolingual margin. The posterior portion is dominated by the large hypoconid closely associated with a small entoconid.

Ecology.—R. labo is known from three localities on the northern slope of Mt. Labo; in montane forest at 1,250 m, transitional montane–mossy forest at 1,335 m, and in mossy forest at 1,413 m elevation (Balete et al. 2013a; this study). It was not trapped at lower elevations in lowland and montane forest between 626 and 1,115 m despite considerable trapping effort. Forest structure and dominant plant groups at survey localities are described elsewhere (Balete et al. 2013a). In addition to

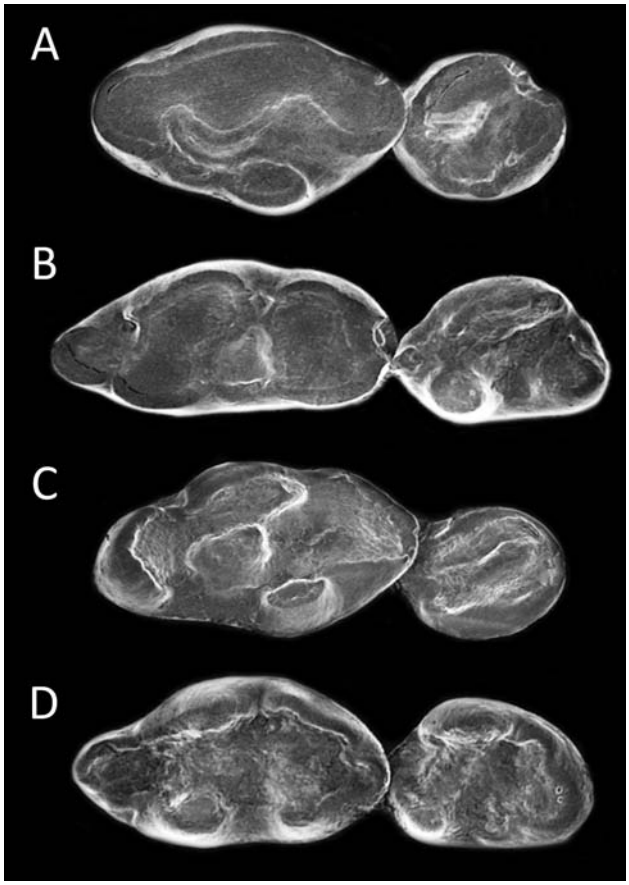

Fig. 8.—Occlusal views of the left maxillary and right mandibular molars of (A and B) *Rhynchomys labo* (FMNH 189833, paratype, young adult); and (C and D) *R. mingan* (FMNH 191058, paratype, juvenile-adult).

R. labo, four other small mammal species occur on Mt. Labo, including three native species: *Apomys microdon* Hollister, 1913; *Rattus everetti* (Günther, 1879); and *Crocidura grayi* Dobson, 1890, and one non-native species: *Suncus murinus* (Linnaeus, 1766); all four species co-occur with *R. labo*. At the localities where it was documented, *R. labo* was either the most abundant or the second most abundant native species. All 23 individuals captured were taken in snap traps set on the ground surface and baited with earthworms. Many were trapped in well-defined runways approximately 10 cm in width beneath dense vegetation and under complete canopy cover. In 2006, trap success for *R. labo* was 3.72% (16 individuals in 440 trap-nights with earthworm bait). In contrast to congeners that principally have nocturnal–crepuscular activity (Rickart et al. 1991, 2011, 2016; Balete and Heaney 1997; Balete et al. 2007), several captures of *R. labo* were during full daylight (Balete et al. 2013a).

Rhynchomys mingan, new species

Mingan shrew-rat

Figs. 7–10, Tables 1 and 2

Rhynchomys sp.: Balete, Alviola, M. R. M. Duya, M. V. Duya, Heaney, and Rickart 2011:80.
Rhynchomys sp.: Heaney, Balete, and Rickart, 2016:163.

Holotype.—Adult male, FMNH 191043, trapped on 29 May 2006 by Danilo S. Balete (original number 4108). The specimen consists of the body fixed in formaldehyde solution and preserved in 70% ethanol, the cleaned skull, and a sample of unfixed muscle tissue from the thigh preserved in 95% ethanol. All parts are in excellent condition. The specimen, now located at the Field Museum, is to be deposited at the Philippine National Museum of Natural History, Manila, Republic of the Philippines.

Type locality.—1.8 km S, 1.0 km W Mingan Peak, Dingalan Municipality, Aurora Province, Luzon Island, Republic of the Philippines, 1,677 m elevation, 15.46586°N, 121.39457°E (Fig. 1; Balete et al. 2011, figure 2A).

Paratypes (n = 22).—Along with the holotype, three additional males and two females were collected at the type locality on 29 May 2006 (FMNH 191042, 191044–19047). Other specimens include two females collected between 12 and 13 June 2006 from 3.5 km S, 1.7 km W Mingan Peak, 1,476 m, 15.46620°N, 121.38846°E (FMNH 191063, 191064); five males and six females collected between 6 and 8 June 2006 from 1.5 km S, 0.5 km W Mingan Peak, 1,681 m, 15.46802°N, 121.40039°E (FMNH 191052–191062); and two males and two females collected between 3 and 4 June 2006 from 0.9 km S, 0.3 km W Mingan Peak, 1,785 m, 15.47390°N, 121.40026°E (FMNH 191048–191051). All specimens were initially preserved in fluid; the skulls of five were later removed and cleaned. Half of the paratypes, now located at the Field Museum, are to be deposited at the Philippine National Museum of Natural History.

Distribution.—Known only from localities in old-growth montane and mossy forest on the southwestern slope of Mt. Mingan between 1,476 and 1,785 m elevation.

Etymology.—The new species is named for the Mingan Mountains where the specimens originated. The specific epithet is used as a noun in apposition. We propose "Mingan shrew-rat" as the English common name.

Nomenclatural statement.—A LSID number was obtained for the new species (*Rhynchomys mingan*): urn:lsid:zoobank.org:act:D4D4B97A-BE03-4F00-8BDB-A350BD44E70B.

Diagnosis.—*R. mingan* is distinguished from other members of the genus as follows: differs from *R. banahao* in having larger body size, shorter pelage, paler venter, larger skull with a longer and narrower rostrum, and smaller upper and lower second molars; differs from *R. tapulao* by its larger body size, shorter and darker pelage, wider skull with relatively broader rostrum, smaller auditory bulla, and larger mandible; differs from *R. isarogensis* by its larger body size, shorter pelage, larger skull with longer and broader rostrum, and a longer mandible; differs from *R. labo* in having larger body size, longer tail, and skull larger in nearly all dimensions; differs from *R. soricoides* in having smaller body size, shorter tail, shorter pelage, smaller skull with a shorter and broader rostrum, shorter incisive foramina, and a shorter mandible. External and cranial features of *R. mingan* are most similar to those of *R. soricoides*. Accordingly, comparisons between these two species are emphasized in the following section.

Description and comparisons.—*R. mingan* (Fig. 9) is a medium-sized murid similar to other members of the genus in general body

Fig. 9.—*Rhynchomys mingan*. Drawing by Velizar Simeonovski.

form and cranial morphology but differing in body size, relative proportions of the limbs and tail, pelage color, and cranial features (Tables 1 and 2; Figs. 4, 6–8, and 10). Head plus body length of *R. mingan* is significantly shorter than in *R. soricoides* ($z = 2.36$, $n_1 = 31$, $n_2 = 18$, $P < 0.01$), but there is no significant difference in weight. The dorsal pelage is dark grayish brown, similar to that of *R. soricoides* and *R. labo*, darker than in *R. tapulao*, and paler than in *R. banahao*. The mid-dorsal overfur is shorter in *R. mingan* than in *R. soricoides*. The venter is medium gray, uniformly paler than the dorsum; similar to that of *R. soricoides* but with paler yellowish-brown highlights. As in *R. soricoides*, most individuals have patches of pure white hair on the throat, chest, abdomen, or a combination of these. Laterally, there is a gradual blending of dorsal and ventral coloration, unlike the abrupt transition seen in *R. tapulao* and *R. labo*.

As in the other species, the lips and rhinarium are unpigmented, and there is a narrow, pale eye ring. The ears of *R. mingan* are shorter than those of *R. soricoides* ($z = 5.23$, $n_1 = 31$, $n_2 = 18$, $P < 0.001$) and are grayish brown with a covering of short hairs; coloration is paler than in the other species, particularly on the inner surface. As in other species, the mystacial vibrissae are long; the thickest and longest (up to 50 mm) are dark brown and extend well beyond the ears. Toward the anterior end of the muzzle, they are progressively shorter, thinner, and paler. Short (5–15 mm) vibrissae are located behind the eyes, and under the jaw and forearm. These less conspicuous vibrissae also are present in the other species of *Rhynchomys*.

The forefeet of *R. mingan* and *R. soricoides* are similar in coloration and pilation. The dorsal and palmar surfaces are unpigmented. A sparse covering of short hairs extends from the wrist down along the medial edge of the foot; these are mainly dark brown, but are unpigmented on the medial side. The forefoot is slightly smaller and the digits more delicate than in *R. soricoides*.

The hind foot of *R. mingan* is absolutely shorter than in *R. soricoides* ($z = 3.44$, $n_1 = 31$, $n_2 = 18$, $P < 0.001$), but not

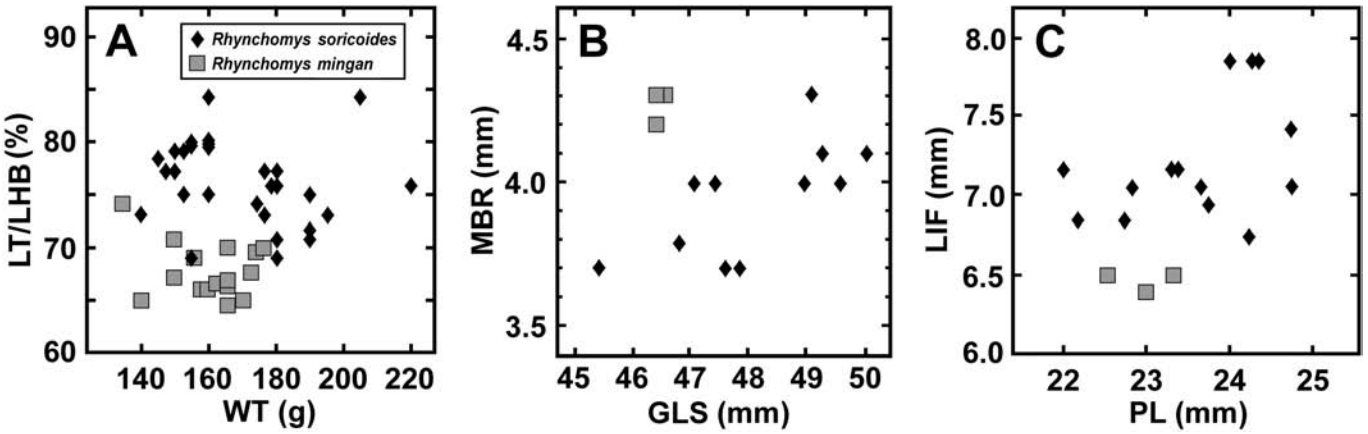

Fig. 10.—Bivariate plots of measurements and measurement ratios comparing *Rhynchomys mingan* and *R. soricoides.* A) Length of tail as a percentage of length of head and body (LT/LHB %) versus body weight (WT). B) Medial breadth of rostrum (MBR) versus greatest length of skull (GLS). C) Length of incisive foramen (LIF) versus palatal length (PL).

relative to the length of head plus body. Except for partially pigmented scale rings on the upper surface of the toes, the dorsal surface of the foot is unpigmented. Scattered short hairs cover the dorsal surface; those on the medial side are unpigmented, with a mixture of dark brown and pale hairs over the remaining surface. Hairs on the lateral sides of the ankle and heel are predominantly dark brown, extending as a thin dark line nearly to the base of the fourth digit. A similar pattern of dorsal coloration on the hind foot is seen in *R. labo*, *R. isarogensis*, and in some specimens of *R. soricoides*, which is geographically variable. The dorsal surface of the foot is uniformly dark gray in *R. banahao*, and uniformly unpigmented in *R. tapulao*. As in the other species, the plantar surface is naked and with pads that are small relative to the size of the foot. The toes, pads, the posterior tip of the heel, and an isolated band between the heel and the thenar are unpigmented; the remainder of the plantar surface is medium gray.

The tail of *R. mingan* is shorter than that of *R. soricoides*, both absolutely ($z = 5.73$, $n_1 = 31$, $n_2 = 18$, $P < 0.001$) and relative to the length of the head plus body ($z = 5.11$, $n_1 = 31$, $n_2 = 18$, $P < 0.001$; Fig. 10A). The tail is longer than that of *R. labo*, but similar in length to those of the remaining species (Table 1). Tail scales on the dorsal surface are dark brownish gray. The underside of the tail is substantially paler than the dorsal surface. Most scales are pale gray, but in all specimens, there is a mid-ventral stripe of darker gray extending from the base of the tail nearly to the tip. Some specimens of *R. soricoides* have a similar pattern of coloration (unpigmented below with a narrow mid-ventral stripe of gray), but in others the ventral surface is uniformly unpigmented, lightly pigmented, or a mosaic of pigmented and unpigmented areas. Other species have tails that are nearly uniformly dark often with an unpigmented tip (*R. banahao* and *R. labo*), or bicolored dorsoventrally (*R. isarogensis*), or baso-distally (*R. tapulao*). Tail scales of both *R. mingan* and *R. soricoides* are large (fewer scale rows per centimeter) compared to those of the other species (Table 1). As in all species, there are three short, stiff hairs adjacent to each scale; the relative length and pigmentation of the hairs generally reflect the size and pigmentation of the adjacent scale.

R. mingan shares the same cranial specializations seen in other members of the genus (Figs. 6 and 7; Balete et al. 2007, figures 4 and 5). The average length of the skull is slightly less than in *R. soricoides*, but greater than in the other species. In the dorsal perspective, the skull appears to be less elongated (relative to its width) than in *R. soricoides*, but slightly more so than in the other species. The rostrum is shorter than in *R. soricoides*, longer than in *R. labo* or *R. isarogensis*, but comparable to those of *R. banahao* and *R. tapulao*. Relative to skull length, the rostrum of *R. mingan* is substantially wider than in *R. soricoides*; a bivariate plot of the medial breadth of the rostrum (MBR) against skull length (GLS) reveals no overlap between the two species (Fig. 10B). In *R. labo*, medial breadth is nearly equal to anterior breadth across the incisor capsules, such that the rostrum lacks the prominent medial constriction seen in the other species. As in the other species, the nasals of *R. mingan* project beyond the premaxillae. The nasal tips are narrower than in *R. soricoides*, but not as acutely pointed as in *R. labo.* The anterior portion of the zygomatic arch is less strongly backswept than in the other species, and the maxillary root does not prominently project forward as in *R. soricoides.* The difference between the ZB and breadth of the braincase is greater than in *R. soricoides*, but not as great as in *R. labo*. The interorbital region is broad, as in *R. banahao* and *R. tapulao*, but substantially more so than in *R. soricoides* and the other species. The braincase is not as long as that of *R. soricoides* but it has a similar posterior margin due to the inflation of the supraoccipital. The dorsal surface of the cranium is entirely smooth and without ridges.

From the lateral perspective (Fig. 7), the rostrum of *R. mingan* appears to be shorter and deeper than that of *R. soricoides*; its general outline is similar to that of the other species although it is not as deep as in *R. isarogensis* (Fig. 6). The nasals project forward well beyond the premaxillae and project dorsad slightly near the tips as they do, to a variable extent, in the other species except for *R. banahao*, in which they are nearly straight. Posteriorly from their tips, the dorsal profile of the skull is nearly straight to a slight bulge over

the frontal sinuses, then smoothly convex over the top of the braincase, flattening over the interparietal to a very slight protuberance at the supraoccipital margin. The occipital margin is moderately inflated with a smooth, rounded profile as in *R. labo* and *R. tapulao*, but not as inflated as in *R. banahao* and *R. isarogensis*. In contrast, the lateral profile of the braincase is quite different in *R. soricoides*; it is flatter dorsally and with a more expanded posterior margin that projects further beyond the occipital condyles (Fig. 7). In *R. mingan*, as in the other species, there is but slight overlap between the dorsal and ventral maxillary roots of the zygomatic arch, imparting a strong posterior slant to the zygomatic plate. The plate is narrower than in *R. soricoides* and *R. labo*, but broader than in *R. tapulao*, and it has a less convex anterior profile compared to the other species except *R. tapulao*, in which the anterior margin is nearly straight. The posterior portion of the squamosal root of the zygomatic arch is just above the postglenoid vacuity, as in the other species. The auditory bulla is about the same height as that of *R. soricoides*, but is shorter. The mastoid of *R. mingan* is moderately inflated as in the other species; it lacks the foramen seen in *R. banahao* and in some specimens of *R. labo*.

In ventral view (Fig. 7), the greater medial breadth of the rostrum of *R. mingan* compared to congeners is most apparent. The interpremaxillary foramen is short and narrow compared to that of *R. soricoides.* LIF is less than in *R. soricoides*, both absolutely and relative to PL; a bivariate plot of these measurements reveals no overlap between the two species (Fig. 10C). The palatine grooves are prominent, as are the postpalatine foramina, but the posterior extension of the grooves beyond the foramina is less conspicuous than in *R. labo* and some specimens of *R. soricoides*. Excepting *R. soricoides*, the palatal bridge is longer than in the other species. The mesopterygoid fossa of *R. mingan* is narrower than in the other species except *R. soricoides*. The auditory bulla is shorter than those of the other species except *R. labo*. The gap separating the bulla from the squamosal and alisphenoid is not as great as in *R. soricoides* or *R. banahao*, but larger than in the other species.

The upper incisors of *R. mingan* are similar in size and conformation to those of congeners. In common with the other species, the maxillary toothrow is very short, consisting only of M1 and M2. As in other species, there is a bony ridge adjacent to the anterolateral margin of M1. This ridge forms a flat shelf that extends well beyond the anterior margin of the tooth in both *R. mingan* and *R. soricoides*; this shelf is not present in either *R. labo* or *R. isarogensis*, and is less developed in the other species. Most specimens of *R. mingan* are adults with molars having moderate to heavy wear on occlusal surfaces; however, one (FMNH 191058) is a young animal (juvenile-adult age class of Musser and Heaney 1992) with nearly unworn molars (Fig. 8C; see also Balete et al. 2007, figure 6; Musser and Heaney 1992, figure 49). As in the other species, M1 is narrow with tapered ends. All of the individual cusps are distinguishable in the juvenile-adult specimen; they form three groups. The anterolingual cusp t1 is missing; the small anterocone consists only of coalesced cusps t2 and t3. The second row includes cusps t4, t5, and t6, all of which are large and distinct. The posterior group consists of cusps t8 and t9, which are coalesced and cannot be distinguished individually. As in the other species of *Rhynchomys*, M2 has a circular occlusal outline and a simplified cusp pattern of two groups; the anterior consists of coalesced t4, t5, and t6, and the posterior consists of an enlarged t8 and tiny t9. The upper molars of the holotype are heavily worn, but they retain the same basic cusp pattern seen in the juvenile-adult, including the prominence of t4 and the absence of t1 on M1. With respect to shape and cusp patterns, the upper molars of *R. mingan* are most similar to those of *R. soricoides*.

The mandible of *R. mingan* is long and slender as in congeners (Fig. 6 and 7; Balete et al. 2007, figure 5). It is appreciably smaller than that of *R. soricoides*, but longer than those of the other species. The posterior portion of the mandible of *R. mingan* is similar to that of *R. soricoides*; in both, the angular process extends posteriorly past the end of the condyloid process, whereas in the other species the posterior extension of these processes is nearly equal. The lower incisors are similar to those of the other species. The lower molars of the juvenile-adult specimen of *R. mingan* show very little wear and reveal complete cusp patterns (Fig. 8D). The m1 is shorter and broader than in *R. soricoides.* The small anteroconid consists of the coalesced anterolingual and anterolabial cusps; the cusps are coalesced but retain distinctive outlines. The large protoconid and metaconid form a second group, and behind these the prominent hypoconid and entoconid comprise a third group. A broad posterior cingulum imparts a rounded posterior tooth margin rather than the tapered margin seen in *R. soricoides* and other species; in *R. banahao*, m1 also has a round posterior margin but this is associated with the absence of a posterior cingulum. The m2 is small as in the other species except *R. banahao*. The anteroconid appears to be small and partially coalesced with the metaconid. The protoconid dominates the labial margin of the tooth. On the posterolabial side, a small hypoconid is closely associated with the posterior margin of the protoconid, while a large ectoconid dominates the posterolingual portion of the tooth. There is no posterior cingulum on m2. Although the holotype of *R. mingan* has considerable tooth wear, m1 retains the same basic outline of the dominant cusps and the broad posterior cingulum seen in the juvenile-adult. The m2 of the holotype has less wear; the cusp pattern is similar to that of the juvenile-adult, except the hypoconid is much larger, resulting in a quadrate rather than rounder posterior margin.

Ecology.—*R. mingan* was recorded at localities in old-growth montane forest (1,476 m elevation) and mossy forest (1,677–1,785 m) along an elevational gradient on the southwestern slope of Mt. Mingan. Photographs and descriptions of habitat at survey localities are found in Balete et al. (2011). *R. mingan* was relatively common where it was recorded, particularly at localities in mossy forest where it was the second or third most abundant species of small mammal (Balete et al. 2011). It was not found at lower elevations on the mountain (559–1,305 m) despite considerable trapping effort. The species appears to be

primarily nocturnal–crepuscular; out of 23 individuals, only one was captured during daytime. Trapping data strongly suggest that *R. mingan* is a ground-dwelling vermivore. All individuals were captured in snap traps baited with earthworms and set on the ground, often in heavily used runways; this despite the fact that some traps were set above ground and nearly half of the trapping effort involved traps baited with coconut and peanut butter. These traits are similar to those reported for other species of *Rhynchomys*. For all localities where *R. mingan* was either captured or inferred to be present (from adjacent records along the elevational gradient), the species-specific trap success for earthworm traps set on the ground was 1.61% (23 captures out of 1,428 trap-nights—Balete et al. 2011). This is slightly higher than success rates reported for other species of *Rhynchomys* (Rickart et al. 1991; Balete 1995; Balete and Heaney 1997; Balete et al. 2007; this study). Eight other species of native, non-volant, small mammals co-occurred with *R. mingan*, including the shrew *Crocidura grayi*, and the murid rodents *Apomys aurorae* Heaney et al., 2011; *A. microdon* Hollister, 1913; *A. minganensis* Heaney et al., 2011; *A. musculus* Miller, 1911; *Bullimus luzonicus* (Thomas, 1895); *Rattus everetti*; and *Soricomys leonardocoi* Balete et al., 2013a. With the exception of *C. grayi* and *R. everetti*, these species are endemic to Luzon, and three (*A. aurorae*, *A. minganensis*, and *S. leonardocoi*) are known only from Mt. Mingan (Balete et al. 2011, 2012).

Discussion

Phylogenetic relationships.—The most comprehensive phylogenetic analysis of the Chrotomyini, based on the entire cytochrome *b* gene and six nuclear loci, revealed a sister relationship between *Rhynchomys* and *Chrotomys* + *Soricomys* (Rowsey et al. 2018; also see Balete et al. 2012). Among the four species of *Rhynchomys* included in that analysis, branch lengths were short, indicating recent diversification (Rowsey et al. 2018, figure 3b). There was high bootstrap support (90–100%) for a sister relationship between *R. soricoides* and *R. tapulao*, weak support (< 75%) for a sister relationship between *R. isarogensis* and *R. banahao*, and complete support (100%) for a sister relationship between these pairs (Rowsey et al. 2018, figures 2b). The morphological data presented here suggest relationships between *R. labo* and *R. isarogensis*, and between *R. mingan* and *R. soricoides*; arrangements that generally are concordant with the molecular data in that apparent species relationships are aligned with geographic region (northern and central Luzon versus southern Luzon).

Biogeography.—At 1,901 m, Mt. Mingan is the highest peak in the Mingan Mountains, which comprise the central portion of the Sierra Madre Range that is separated from adjacent highland areas by deep river valleys with elevations below 500 m (Fig. 1; Balete et al. 2011). The isolation and topographic complexity of this region have produced a fauna rich in endemic species; among the nine species of small, non-volant mammals documented on Mt. Mingan, *R. mingan* is one of four species known only from the mountain (Balete et al. 2011). Furthermore, *R. mingan* is the only species in the genus known from the Sierra Madre chain. The fact that faunal surveys conducted elsewhere in the Sierra Madre system (Danielsen et al. 1994; Duya et al. 2011; Balete et al. 2013b; Heaney et al. 2013) did not document *Rhynchomys*, suggests that the distribution of the genus within the Sierra Madre complex may be restricted to the Mt. Mingan highlands. Additional surveys elsewhere in the Sierra Madre system certainly are warranted.

Mt. Labo is one of several volcanic peaks on the Bicol Peninsula that formed a series of isolated islands beginning about 6.6 Ma that increased in number and area 2–3 Ma, resulting in a chain of stratovolcanoes separated by intervening lowlands (Heaney et al. 2016). The historical biogeography of small mammals in the Bicol region is correspondingly complex, involving early dispersal across water barriers followed by isolation and divergence, and later arrival of widespread species (Heaney et al. 2016; Kyriazis et al. 2017). Mt. Isarog (1,966 m) in the central portion of the peninsula supports a small mammal fauna that includes eight native non-volant species, of which there are locally endemic species belonging to four murid genera (Rickart and Heaney 1991; Rickart et al. 1991; Heaney et al. 1999; Balete et al. 2015). In contrast, the fauna of Mt. Labo (1,544 m) is comparatively depauperate, consisting of four native species including one that is locally endemic (*R. labo*) and three that are widespread (Balete et al. 2013a). The two mountains are separated by approximately 60 km of intervening lowland below 500 m elevation (Fig. 1). Our results show that *R. labo* and *R. isarogensis* are morphologically distinct but share certain features that distinguish them from congeners (e.g., small size, craniodental similarities). We hypothesize that they share a common ancestor that dispersed to the Bicol region prior to the coalescence of the peninsula with central and northern Luzon (Heaney et al. 2016). Additional field surveys elsewhere in the Bicol Peninsula would increase our understanding of the complex biogeography of this region (Balete et al. 2013a).

Conservation.—In common with the other species of *Rhynchomys*, *R. labo* and *R. mingan* are restricted to mid to high elevations in montane and mossy forest habitats that have minimal anthropogenic disturbance. Nonetheless, all areas of highland habitat, and particularly those supporting endemic species, require protection from direct overexploitation of forest resources and indirect threats posed by geothermal development and mining activities. Protection of these areas would have added socioeconomic benefit in maintaining crucial watershed functions in this region of frequent typhoons.

Acknowledgments

For assistance with Field Museum expeditions to Mt. Labo and Mt. Mingan, we thank J. Sarmiento, M. R. M. Duya, M. V. Duya, R. Altamirano, L. Co, U. Ferras, N. Bartolome, F. Dalen, G. Bueser, B. Soriano, and R. Fernandez. During the 2008 University of Kansas field expedition to Mt. Labo, N. Antoque, R. Brown, J. Cantil, P. Hosner, and C. Siler made outstanding contributions. The Biodiversity Management

Bureau (formerly the Protected Areas and Wildlife Bureau), Philippine Department of Environment and Natural Resources, provided scientific study permits; we owe special thanks to T. M. Lim, J. de Leon, C. Custodio, A. Manila, M. Mendoza, and A. Tagtag. For their assistance working with specimens, we thank A. Ferguson, J. Phelps, W. Stanley, and M. Schulenberg (FMNH), M. Eifler (KU), and B. Hamel (UMNH). We thank D. Lunde for the loan of USNM specimens of *R. isarogensis*. B. Strack and L. Ui'Dhalaigh assisted with the preparation of SEM images at FMNH. We thank N. Slade for advice on statistical methods. Finally, we thank P.-H. Fabre and two anonymous reviewers for their helpful suggestions and comments on the manuscript. Funding for fieldwork and laboratory research was provided by the National Science Foundation (DEB-0743491 to R. Brown), Conservation International–Philippines, the Negaunee Foundation, the Grainger Foundation, the Field Museum's Barbara Brown Fund for Mammal Research, Marshall Field Fund, and Ellen Thorne Smith Fund.

Supplementary Data

Supplementary data are available at *Journal of Mammalogy* online.

Supplementary Data SD1.—Variable loadings, eigenvalues, and percent variance explained on the first four components of a principal components analysis of 20 $\log_{10}$-transformed cranial measurements of adult specimens of *Rhynchomys banahao*, *R. isarogensis*, *R. labo*, *R. mingan*, *R. soricoides*, and *R. tapulao*. Variable abbreviations are defined in "Materials and Methods" section.

Supplementary Data SD2.—Variable loadings, eigenvalues, and percent variance explained on the first four components of a principal components analysis of 12 $\log_{10}$-transformed cranial measurements of adult *Rhynchomys banahao*, *R. isarogensis*, and *R. labo*. Variable abbreviations are defined in "Materials and Methods" section.

Supplementary Data SD3.—Variable loadings, eigenvalues, and percent variance explained on the first four components of a principal components analysis of 12 $\log_{10}$-transformed cranial measurements of adult *Rhynchomys mingan*, *R. soricoides*, and *R. tapulao*. Variable abbreviations are defined in "Materials and Methods" section.

Literature Cited

Balete, D. S. 1995. Population ecology of small mammals in the mossy forest of Mt. Isarog, southern Luzon, Philippines. M.S. thesis, University of Illinois, Chicago.

Balete, D. S., P. A. Alviola, M. R. M. Duya, M. V. Duya, L. R. Heaney, and E. A. Rickart. 2011. The mammals of the Mingan Mountains, Luzon: evidence for a new center of mammalian endemism. Fieldiana: Life and Earth Sciences 2:75–87.

Balete, D. S., and L. R. Heaney. 1997. Density, biomass, and movement estimates for murid rodents in mossy forest on Mount Isarog, southern Luzon, Philippines. Ecotropica 3:91–100.

Balete, D. S., L. R. Heaney, P. A. Alviola, and E. A. Rickart. 2013a. Diversity and distribution of small mammals in the Bicol Volcanic Belt of southern Luzon Island, Philippines. National Museum of the Philippines: Journal of Natural History 1:61–86.

Balete, D. S., L. R. Heaney, and E. A. Rickart. 2013b. The mammals of Mt. Irid, Southern Sierra Madre, Luzon Island. National Museum of the Philippines: Journal of Natural History 1:15–29.

Balete, D. S., et al. 2012. *Archboldomys* (Muridae: Murinae) reconsidered: a new genus and three new species of shrew mice from Luzon Island, Philippines. American Museum Novitates 3754:1–60.

Balete, D. S., E. A. Rickart, L. R. Heaney, and S. A. Jansa. 2015. A new species of *Batomys* from southern Luzon Island, Philippines. Proceedings of the Biological Society of Washington 128:22–39.

Balete, D. S., E. A. Rickart, R. G. B. Rosell-Ambal, S. Jansa, and L. R. Heaney. 2007. Descriptions of two new species of *Rhynchomys* Thomas (Rodentia: Muridae: Murinae) from Luzon Island, Philippines. Journal of Mammalogy 88:287–301.

Brown, J. C. 1971. The description of mammals–1. The external characters of the head. Mammal Review 1:151–168.

Brown, J. C., and D. W. Yalden. 1973. The description of mammals–2. Limbs and locomotion of terrestrial mammals. Mammal Review 3:107–134.

Burgin, C. J., J. P. Colella, P. L. Kahn, and N. S. Upham. 2018. How many species of mammals are there? Journal of Mammalogy 99:1–14.

Danielsen, E., et al. 1994. Conservation of biological diversity in the Sierra Madre Mountains of Isabela and southern Cagayan Province, the Philippines. BirdLife International, Manila, Philippines.

Duya, M. R. M., M. V. Duya, P. A. Alviola, D. S. Balete, and L. R. Heaney. 2011. Diversity of small mammals in montane and mossy forests on Mount Cetaceo, Cagayan Province, Luzon. Fieldiana: Life and Earth Sciences 2:88–95.

Esselstyn, J. A., A. S. Achmadi, and K. C. Rowe. 2012. Evolutionary novelty in a rat with no molars. Biology Letters 8:990–993.

Heaney, L. R., D. S. Balete, P. A. Alviola, M. R. M. Duya, and E. A. Rickart. 2013. The mammals of Mt. Anacuao, NE Luzon Island, Philippines: a test of predictions of Luzon small mammal diversity patterns. National Museum of the Philippines: Journal of Natural History 1:1–13.

Heaney, L. R., D. S. Balete, and E. A. Rickart. 2016. The mammals of Luzon: biogeography and natural history of a Philippine fauna. Johns Hopkins University Press, Baltimore, Maryland.

Heaney, L. R., D. S. Balete, E. A. Rickart, R. C. B. Utzurrum, and P. C. Gonzales. 1999. Mammalian diversity on Mount Isarog, a threatened center of endemism on southern Luzon Island, Philippines. Fieldiana: Zoology 95:1–62.

Jansa, S. A., F. K. Barker, and L. R. Heaney. 2006. The pattern and timing of diversification of Philippine endemic rodents: evidence from mitochondrial and nuclear gene sequences. Systematic Biology 55:73–88.

Kyriazis, C. C., J. M. Bates, and L. R. Heaney. 2017. Dynamics of genetic and morphological diversification in an incipient intra-island radiation of Philippine rodents (Muridae: *Bullimus*). Journal of Biogeography 44:2585–2594.

Lidicker, W. Z., Jr. 1968. A phylogeny of New Guinea rodent genera based on phallic morphology. Journal of Mammalogy 49:609–643.

Lidicker, W. Z., Jr., and P. V. Brylski. 1987. The conilurine rodent radiation of Australia, analyzed on the basis of phallic morphology. Journal of Mammalogy 68:617–641.

Musser, G. G., and M. D. Carleton. 2005. Superfamily Muroidea. Pp. 894–1531 in Mammal species of the world, a taxonomic and geographic reference. 3rd ed. (D. E. Wilson and D. M. Reeder, eds.), Johns Hopkins University Press, Baltimore, Maryland.

Musser, G. G., and P. W. Freeman. 1981. A new species of *Rhynchomys* (Muridae) from the Philippines. Journal of Mammalogy 62:154–159.

Musser, G. G., and L. R. Heaney. 1992. Philippine rodents: definitions of *Tarsomys* and *Limnomys* plus a preliminary assessment of phylogenetic patterns among native Philippine murines (Murinae, Muridae). Bulletin of the American Museum of Natural History 211:1–138.

Rickart, E. A., D. S. Balete, P. A. Alviola, M. J. Veluz, and L. R. Heaney. 2016. The mammals of Mt. Amuyao: a richly endemic fauna in the Central Cordillera of northern Luzon Island, Philippines. Mammalia 80:579–592.

Rickart, E. A., and L. R. Heaney. 1991. A new species of *Chrotomys* (Rodentia: Muridae) from Luzon Island, Philippines. Proceedings of the Biological Society of Washington 104:387–398.

Rickart, E. A., L. R. Heaney, D. S. Balete, and B. S. Tabaranza, Jr. 2011. Small mammal diversity along an elevational gradient in northern Luzon, Philippines. Mammalian Biology 76:12–21.

Rickart, E. A., L. R. Heaney, and R. C. B. Utzurrum. 1991. Distribution and ecology of small mammals along an elevational transect in southeastern Luzon, Philippines. Journal of Mammalogy 72:458–469.

Rowe, K. C., A. S. Achmadi, and J. A. Esselstyn. 2016. Repeated evolution of carnivory among Indo–Australian rodents. Evolution 70:653–665.

Rowe, K. C., M. L. Reno, D. M. Richmond, R. M. Adkins, and S. J. Steppan. 2008. Pliocene colonization and adaptive radiations in Australia and New Guinea (Sahul): multilocus systematics of the old endemic rodents (Muroidea: Murinae). Molecular Phylogenetics and Evolution 47:84–101.

Rowsey, D.M., L. R. Heaney, and S. A. Jansa. 2018. Diversification rates of the "Old Endemic" murine rodents of Luzon Island, Philippines are inconsistent with incumbency and ecological opportunity. Evolution 77:1420–1435.

Schenk, J. J., K. C. Rowe, and S. J. Steppan. 2013. Ecological opportunity and incumbency in the diversification of repeated continental colonizations by muroid rodents. Systematic Biology 62:837–864.

Sikes, R. S., and The Animal Care and Use Committee of the American Society of Mammalogists. 2016. 2016 guidelines of the American Society of Mammalogists for the use of wild mammals in research and education. Journal of Mammalogy 97:663–688.

SPSS Inc. 2000. SYSTAT 10. SPSS Inc., Chicago, Illinois.

Steppan, S., R. Adkins, and J. Anderson. 2004. Phylogeny and divergence-date estimates of rapid radiations in muroid rodents based on multiple nuclear genes. Systematic Biology 53:533–553.

Thomas, O. 1895. Preliminary diagnoses of new mammals from northern Luzon, collected by Mr. John Whitehead. Annals and Magazine of Natural History (Series 6) 16:160–164.

Thomas, O. 1898. On the mammals collected by Mr. John Whitehead during his recent expedition to the Philippines. Transactions of the Zoological Society of London 14:377–414.

Submitted 26 July 2018. Accepted 20 March 2019.

Associate Editor was Luis Ruedas.

Appendix

Specimens Examined.—The specimens examined in this study are housed at the Field Museum of Natural History, Chicago, IL (FMNH; n = 82), National Museum of Natural History, Smithsonian Institution, Washington, DC (USNM; n = 28), and Natural History Museum, University of Kansas, Lawrence, KS (KU; n = 6). All localities are on Luzon Island, Republic of the Philippines.

Rhynchomys banahao (*n* = 4).—Quezon Province, Tayabas Municipality, Barangay Lalo, Mt. Banahaw, elev. 1465 m (14°03′59.4″N, 121°30′29.9″E; FMNH 178429, holotype), elev. 1250 m (14°03′N, 121°30′E; FMNH 183590); Laguna Province, Majayjay Municipality, 1.0 km N, 0.4 km E Mt. Banahaw peak, elev. 1625 m (14.07706° N, 121.49262° E; FMNH 218403, 218404).

Rhynchomys isarogensis (*n* = 31).—Camarines Sur Province, Mt. Isarog, 4.5 km N, 20.5 km E Naga, elev. 1125 m (13°40′N, 123°21′E; USNM 573901); 4 km N, 21 km E Naga, elev. 1350 m (13°40′N, 123°22′E; USNM 573573–573575, 573903, 573904); 4 km N, 21.5 km E Naga, elev. 1550 m (13°40′N, 123°22′E; USNM 473578); 4 km N, 22 km E Naga, elev. 1750 m (13°49′N, 123°22′E; USNM 573579–573585, 573900, 573901, 573905-573909, 573911–573915, 573917, 573918); Mt. Isarog, 8.9 km N, 0.8 km E Ocampo Municipality, elev. 1700–1800 m (13°38′32″N, 122°23′30″E; FMNH 147183, 152038); Mt. Isarog, Pili Municipality, Barangay Curry, elev. 5500 ft (FMNH 95123, holotype)

Rhynchomys soricoides (*n* = 35).—Benguet Province, Mt. Pulag National Park, 0.8 km S, 0.9 km W Mt. Babadak peak, elev. 2285 m (16.57299°N, 120.87432°E; FMNH 198790, 198885); 0.8 km S, 0.4 km W Mt. Babadak peak, elev. 2420 m, (16.57361°N, 120.87879°E; FMNH 198883); Babadak Ranger Station, elev. 2445 m (16.57428°N, 120.87812°E; 198784–198788); 0.5 km S, 0.4 km W Mt. Babadak peak, elev. 2480 m (16.57645°N, 120.87830°E; FMNH 198789, 198886, 198887); 1.75 km S, 0.9 km E Mt. Pulag peak, elev. 2650 m (16.58363°N, 120.90512°E; FMNH 198791, 198792); 1.15 km S, 1.35 km E Mt. Pulag peak, elev. 2695 m (15.58816°N, 120.90960°E; FMNH 198783). Kalinga Province, Balbalan Municipality, Barangay Balbalasang, Magdallao, elev. 1600 m (17°27.5′N, 122°04.25′E; FMNH 167320–167322, 167325); Amlicao, elev. 1800 m (17°26′30″N, 121°04′15″E; FMNH 169170, 169174, 169175, 170980, 170981); Mt. Bali-it, elev. 2150 m (17°25.7′N, 120°59.8′E; FMNH 175617,175619). Mountain Province, Barlig Municipality 1.0 km N, 1.0 km W Mt. Amuyao peak, elev. 2100 m (17.02213°, 121.11791°E; FMNH 193836, 214423); Mt. Amuyao peak, elev. 2690 m (17.0133°N, 121.12807°E; FMNH 193829, 193830, 193832, 193835, 193837, 193980); Mt. Data (FMNH 62289, 62290).

Rynchomys tapulao (*n* = 3).—Zambales Province, Palauig Municipality, Barangay Dampay-Salasa, Mt. Tapulao peak, elev. 2024 m (15°24′54.8″N, 120°07′10.4″E; FMNH 183553, 183554, 183555 [holotype]).

Rhynchomys labo (*n* = 22).—See "new species" description above.

Rhynchomys mingan (*n* = 23).—See "new species" description above.